NASA Contractor Report 185292

Rapid Mix Concepts for Low Emission Combustors in Gas Turbine Engines

Milind V. Talpallikar and Clifford E. Smith
CFD Research Corporation
Huntsville, Alabama

Ming-Chia Lai
Wayne State University
Detroit, Michigan

October 1990

NASA

National Aeronautics and
Space Administration

PREFACE

This report is the Phase I Final Report under SBIR Contract NAS3-25834. This report first presents background information and states the approach and objectives of the project. Next, the work performed during the project is discussed, including CFD code modifications, analysis of conventional mixer designs, analysis of Asymmetric Jet Penetration (AJP) designs, and comparison of mixer designs. At the end of the report, conclusions and recommendations for Phase II are stated.

SUMMARY

NASA LeRC has identified the Rich burn/Quick-mix/Lean burn (RQL) combustor as a potential gas turbine combustor concept to reduce NO_x emissions in High Speed Civil Transport (HSCT) aircraft. To demonstrate reduced NO_x levels, NASA LeRC soon will test a flametube version of an RQL combustor. The critical technology needed for the RQL combustor is a method of quickly mixing combustion air with rich burn gases. In this SBIR project, two concepts have been proposed to enhance jet mixing in a circular cross-section:

    1)   the Asymmetric Jet Penetration (AJP) concept; and
    2)   the Lobed Mixer (LM) concept.

In Phase I, two preliminary configurations of the AJP concept were compared with a conventional 12-jet radial-inflow slot design. The configurations were screened using an advanced 3-D Computational Fluid Dynamics (CFD) code named REFLEQS. Both non-reacting and reacting analyses were performed. For an objective comparison, the conventional design was optimized by parametric variation of the jet-to-mainstream momentum flux (J) ratio. The optimum J was then employed in the AJP simulations.

Results showed that the three-jet AJP configuration was superior in overall mixedness compared to the conventional design. However, in regards to NO_x emissions, the AJP configuration was inferior. The higher emission level for AJP was caused by a single "hot" spot located in the wake of the central jet as it entered the combustor. Ways of maintaining good mixedness while eliminating the hot spot have been identified for Phase II study.

Overall, Phase I showed the viability of using CFD analyses to evaluate quick-mix concepts. A high probability exists that advanced mixing concepts will reduce NO_x emissions in RQL combustors, and should be explored in Phase II, by parallel numerical and experimental work.

TABLE OF CONTENTS

1. INTRODUCTION

In order to meet the growing need for faster transportation, High-Speed Civil Transport (HSCT) aircraft and associated propulsion systems have been under study in recent years. One major concern that has surfaced concerning HSCT engines is their impact on deteriorating the earth's ozone layer. Using current technology, a fleet of HSCT aircraft would produce large amounts of oxides of nitrogen (NO_x) while cruising in the stratosphere. Such high levels of NO_x, through a series of well known reactions, would drastically reduce ozone levels. In order to reduce NO_x emissions, technology must be developed to design advanced, low emission combustors. In the late 1970's and early 1980's, low emission technologies were developed for aircraft, industrial and automotive gas turbine applications. By utilizing such technology, a ten-fold reduction in NO_x emission levels (*e.g.* emission index between 3 and 8) may be possible for future HSCT propulsion systems. Emissions research currently being performed at NASA LeRC is aimed at developing the necessary combustion technologies to verify such low emissions.

NO_x is typically formed in gas turbine combustors in two ways: prompt NO_x and thermal NO_x. Prompt NO_x is produced by fast reactions and super-equilibrium concentrations of *O*, *N*, and *OH* in the reaction zone of the combustor. It is essentially uncontrollable, but because its levels are low (emission index between 0 and 1), it does not present a major concern.

However, it is very important to control thermal NO_x. Thermal NO_x is formed in the post-reaction, high temperature region of combustion by slow reactions such as:

$$N + O_2 \leftrightarrow NO + O$$

$$N_2 + 3O \leftrightarrow 2\,NO + O$$
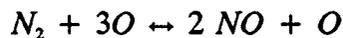
It can be controlled by reducing the reaction temperature/local equivalence ratio (*e.g.* lean burning). Figure 1 shows the effects of flame temperature on NO_x emission index for an ideal, premixed-prevaporized combustor [1].

Two combustor concepts have evolved that rely on uniform lean burning to reduce thermal NO_x. These are: 1) the Lean Premixed/Prevaporized (LPP) concept; and 2) the

Rich burn/Quick-mix/Lean burn (RQL) concept (see Figure 2). The LPP concept premixes and prevaporizes the fuel and air upstream of the combustion zone, thus giving uniformly low flame temperatures during reaction. The overall equivalence ratio in the combustion zone is typically between 0.5 and 0.7. This concept is attractive due to its simplicity. However, potential disadvantages include narrow stability limits and susceptibility to autoignition/flashback.
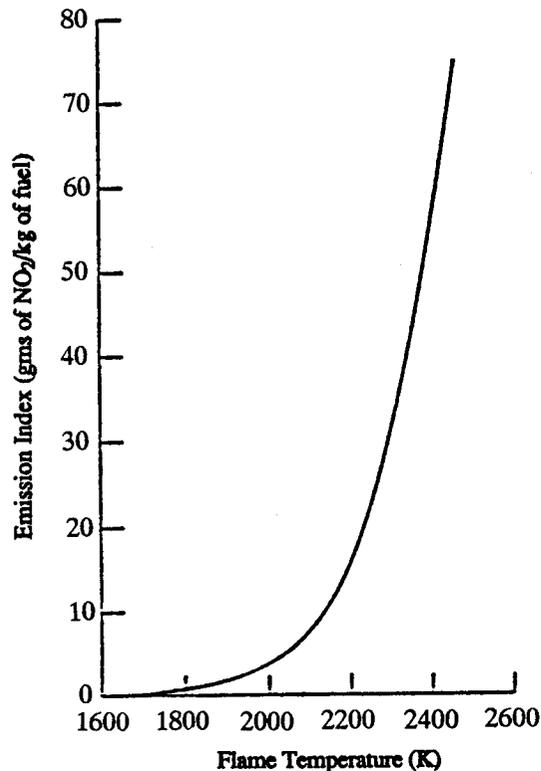
Figure 1. Effect of Flame Temperature on NO_x Emission Index

The RQL concept utilizes staged burning. Combustion is initiated in a fuel rich zone at equivalence ratios between 1.2 and 1.8, thereby eliminating NO_x formation by depleting the available oxygen. Bypass combustion air is introduced in a quick-mix section and lean combustion occurs downstream at an overall equivalence ratio between 0.5 and 0.7. The quick-mix section has a smaller geometric cross-section area than the rich burn zone in order to prevent backflow and enhance mixing. Although more complex than the LPP, the RQL concept offers improved stability, and flame flashback is eliminated as a problem.

COMBUSTION ZONE

COMBUSTION AIR

INSTRUMENTATION

FUEL INJECTOR

PREMIX/PREVAP

FUEL

a) Lean Premixed/Prevaporized (LPP) Concept

Rich Burn Zone

Fuel Preparation Device

Quick Quench Device

Convective Cooling Passage

Lean Burn Zone
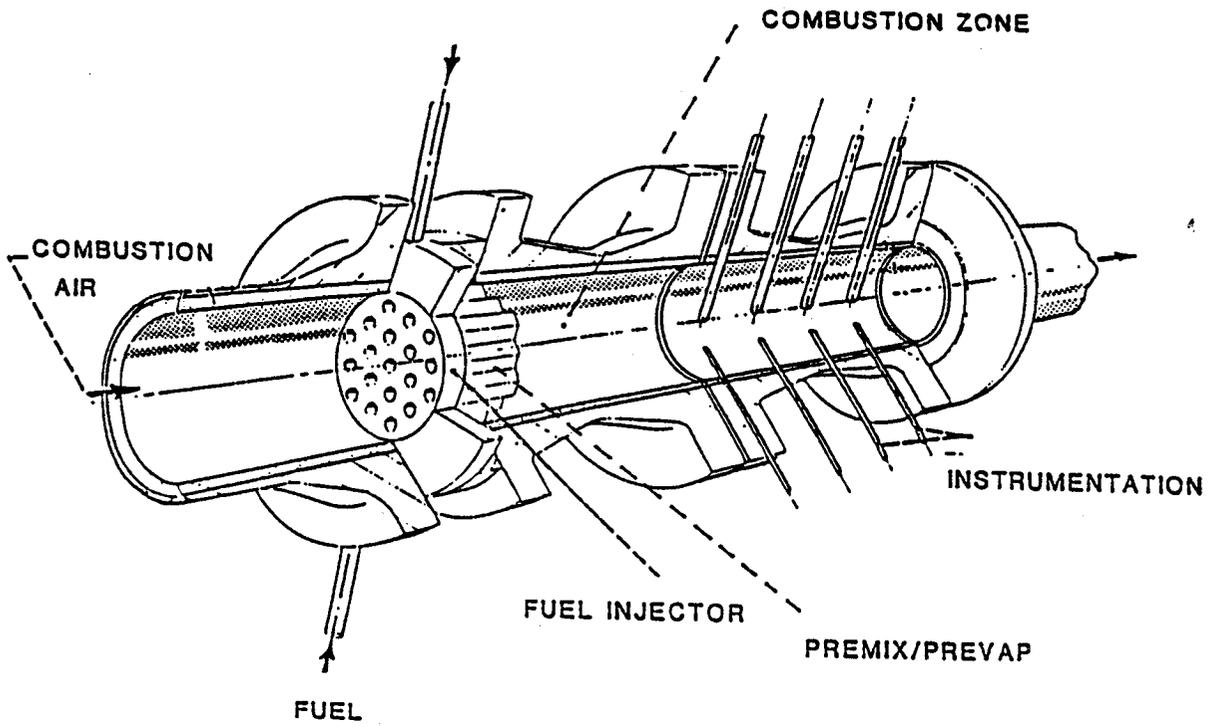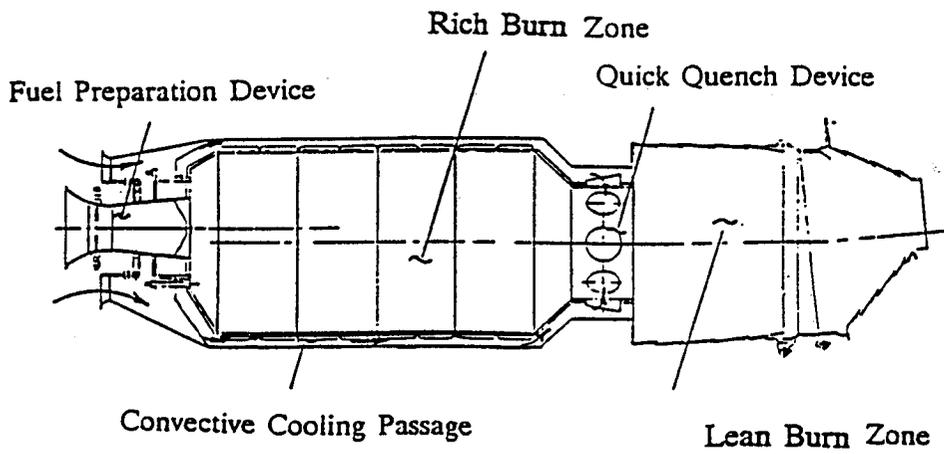
b) Rich Burn/Quick Quench/Lean Burn (RQL) Concept

Figure 2. Two Low NO$_x$ Combustor Concepts

Perhaps the single most important technology need for the RQL concept is how to design the quick-mix section. For previous laboratory combustors, Tacina [2] has shown RQL NO_x levels to be higher than LPP NO_x levels. The higher NO_x emissions for RQL was attributed to stoichiometric burning in the quick-mix section, thus emphasizing the need for innovative rapid mix concepts. Indeed, Nguyen et al. [3] have shown that if instantaneous mixing is assumed in the quick-mix section, low NO_x emission index can be obtained at HSCT cruise flight condition. Hence, the challenge of the RQL concept is to identify quick-mix sections with rapid mixing.

This project seeks to investigate innovative concepts with the potential of enhancing mixing in the quick-mix section of a RQL flametube combustor soon to be tested at NASA LeRC. Conventionally, air has been introduced through radial inflow holes or slots, as shown in Figure 3. According to Holdeman's correlation [4], optimum mixing occurs when the jet penetrates to 0.7 radius into the combustor. The optimum mixing correlation is expressed by the following equation:

$$n = \pi \frac{\sqrt{2J}}{C}$$

where

n   =   optimum number of holes

C   =   experimentally derived constant ~2.5

J   =   jet-to-mainstream momentum flux ratio $(\rho_j V_j^2 / \rho_\infty V_\infty^2)$.

Twelve slots are currently being proposed for the NASA LeRC quick-mix section, thus giving an optimum momentum flux ratio (J) of 46.

Two new concepts are proposed in this project for more rapid mixing in circular cross-sections, consisting of:

1. the Asymmetric Jet Penetration (AJP) concept; and
2. the Lobed Mixer (LM) concept.

In Phase I, only conventional and AJP concepts were studied due to time and cost constraints. Two designs of the AJP concept are shown schematically in Figure 4.
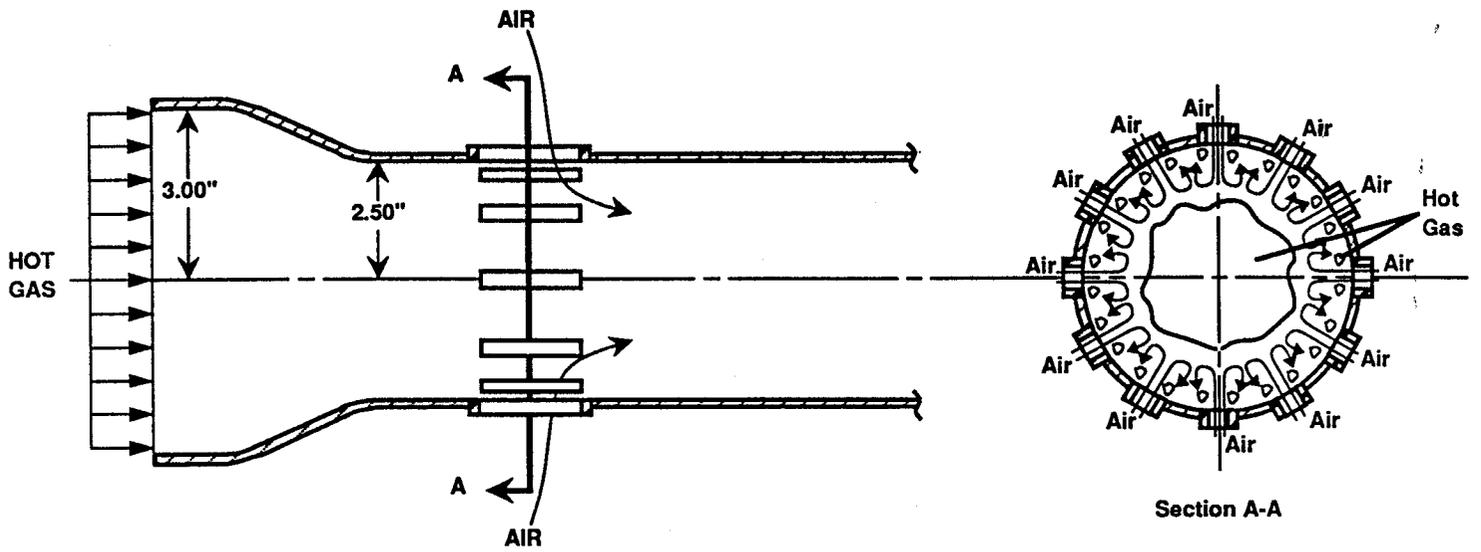
Figure 3. Conventional Quick-Mix Configuration

a) One-Jet

b) Three-Jet
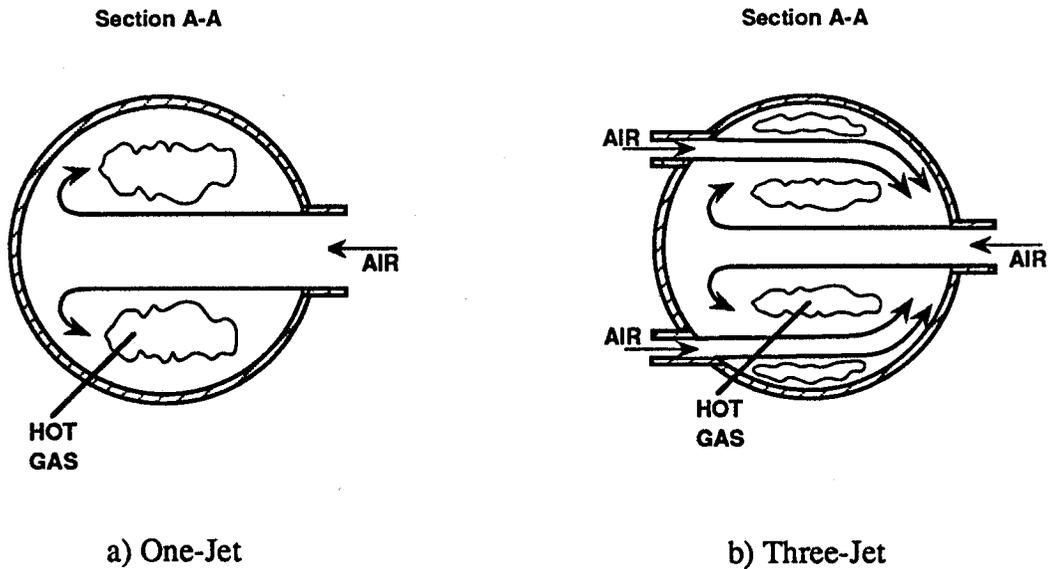
Figure 4. Two Schemes of the Asymmetric Jet Penetration (AJP) Concept

4090/1-001CAB

5

Conventional mixer concepts prohibit jets from penetrating past the centerline, while the AJP concept relies on full jet penetration across the circular cross-section. In many ways, conventional and AJP concepts are comparable to opposed, inline and opposed, staggered holes, respectively, in annular gas turbine combustors. Optimum mixing in annular combustors occurs for opposed, staggered holes when the jets penetrate across the duct to the opposite liner. The AJP concept is a way of utilizing staggered hole technology in can geometries.

2.   PHASE I OBJECTIVES AND APPROACH

The overall goal of Phase I was to show the viability of using 3-D CFD methods to evaluate innovative quick-mix concepts. To this end, two AJP configurations and an optimized conventional scheme were analyzed and evaluated. Specific objectives were:

1. to obtain a 3-D numerical solution of an optimum conventional quick-mix design for NASA LeRC's RQL flametube combustor;
2. to perform 3-D numerical simulations of two AJP schemes; and
3. to compare and assess the AJP concept with the conventional configuration.

All objectives have been satisfied during the course of work in Phase I.

An advanced CFD code, REFLEQS, was used to analyze the quick-mix concepts. REFLEQS was developed by CFDRC to analyze turbulent, reacting flows [5,6]. Its capabilities/methodologies include:

1. solution of two and three-dimensional Navier-Stokes equations for incompressible and compressible flows;
2. cartesian, polar, and non-orthogonal body-fitted coordinates;
3. porosity-resistivity technique for flows with internal blockages;
4. fully implicit and conservative formulation;
5. three differencing schemes: upwind, hybrid, and central differencing with damping terms;
6. standard [7] and extended [8] k-ϵ turbulence models, the two-scale turbulence model of Chen [9], and the low-Reynolds number k-ϵ model of Chien [10];

7. instantaneous, one-step, and two-step combustion models;

8. modified form of Stone's Strongly Implicit Solver; and

9. pressure-based solution algorithms including SIMPLE and a variant of SIMPLEC.

REFLEQS has undergone a considerable amount of systematic quantitative validation for both incompressible and compressible flows. Over 30 validation cases have been performed to data, and good-to-excellent agreement between data and predictions has been shown [11-13].

Two validation cases of the most relevance to this project are those from Garrett's Dilution Jet Mixing Program for NASA LeRC [14]. These cases, whose geometry and flow conditions are described in Figure 5, have opposed, staggered dilution holes with hole spacings and jet momentum flux ratios similar to that of small gas turbine combustors. Temperature measurements and numerical predictions are shown in Figures 6 and 7. Good overall agreement between calculations and measurements can be seen. The good agreement gives confidence in the computed results of this Phase I study.

3. CODE MODIFICATIONS

The REFLEQS code had most of the capabilities needed for this Phase I study. However, a number of modifications/additions were necessary to model the quick-mix concepts. These modifications are discussed below.

3.1 REFLEQS Preprocessor

Several modifications were made to the REFLEQS Preprocessor to handle complex 3-D BFC geometries typical of quick-mix sections.

1. The grid generation 3-D package in the preprocessor was modified to model quick-mix geometries. The modeling of different kinds of slots (e.g. axial slots, transverse slots, slanted slots etc.) was included in the code. Also implemented was an automated non-uniform mesh generation that had previously been used in 2-D but not in 3-D.
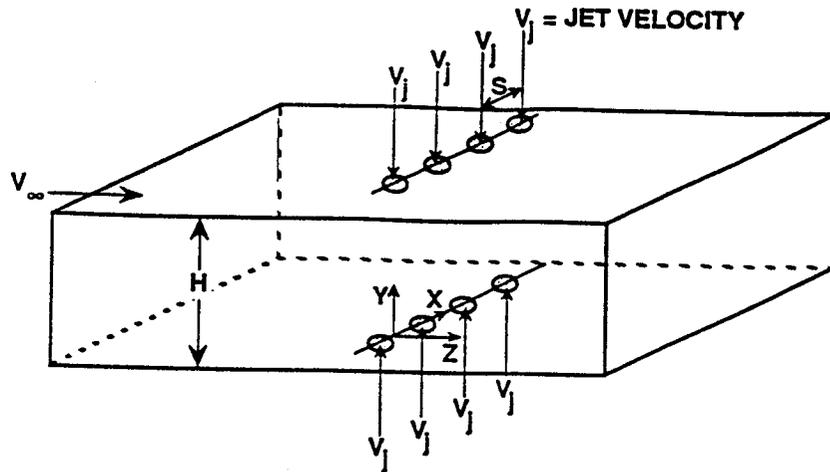
S   = Hole Spacing
D   = Hole Diameter
H   = Test Section Height
V_j = Jet Velocity (m/s)
T_j = Jet Temperature (°K)
V_∞ = Mainstream Velocity (m/s)
T_∞ = Mainstream Temperature (°K)
J   = Jet Momentum Flux Ratio ($\rho_j V_j^2 / \rho_\infty V_\infty^2$)
M   = Mass Flow Ratio ($\Sigma \dot{m}_j / \dot{m}_\infty$)

CASE NO.	ORIFICE CONFIGURATION	ORIFICE DIA (cm)	S/D	H/D	V_j	T_j	V_∞	T_∞	J
1	Opposed Staggered	1.27	4.0	8.0	110	318	16	646	103
2	Opposed Staggered	2.54	4.0	4.0	59	307	17	645	26

Figure 5. Validation Cases from Reference 14

Experimental

Contour	$\dfrac{T_{main} - T}{T_{main} - T_j}$
4	0.20
5	0.25
6	0.32
7	0.35
8	0.40
9	0.45

J = 103
M = 0.47
S/H = 0.5

Numerical

Z/H = 0.25

Z/H = 0.50

Z/H = 0.25
(in plane of jet)

Z/H = 0.50
(in plane of jet)

O data
— REFLEQS

Y/H

Y/H

$\dfrac{T_{main} - T}{T_{main} - T_j}$

$\dfrac{T_{main} - T}{T_{main} - T_j}$
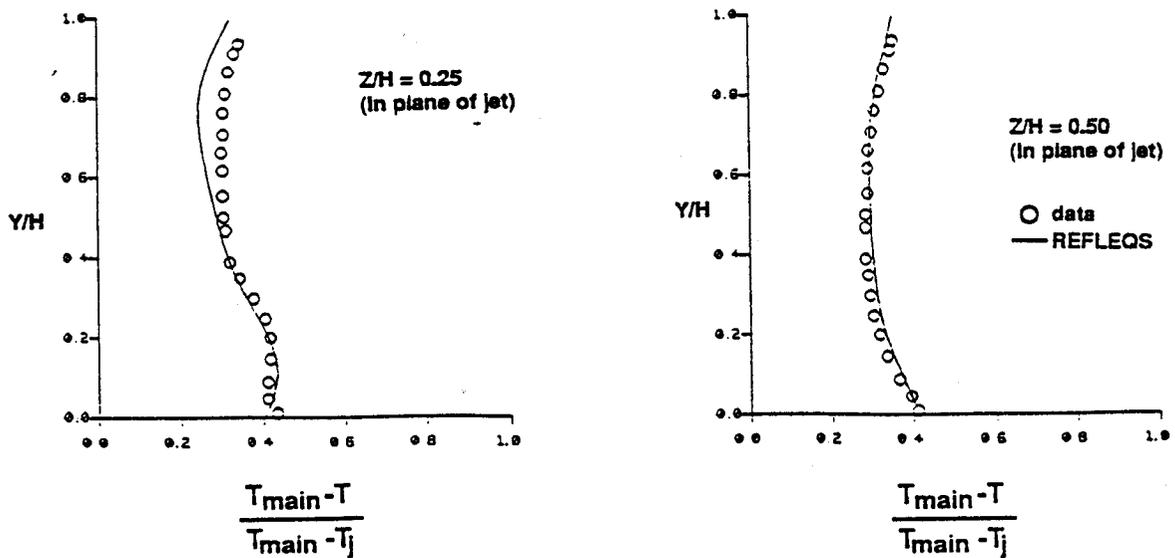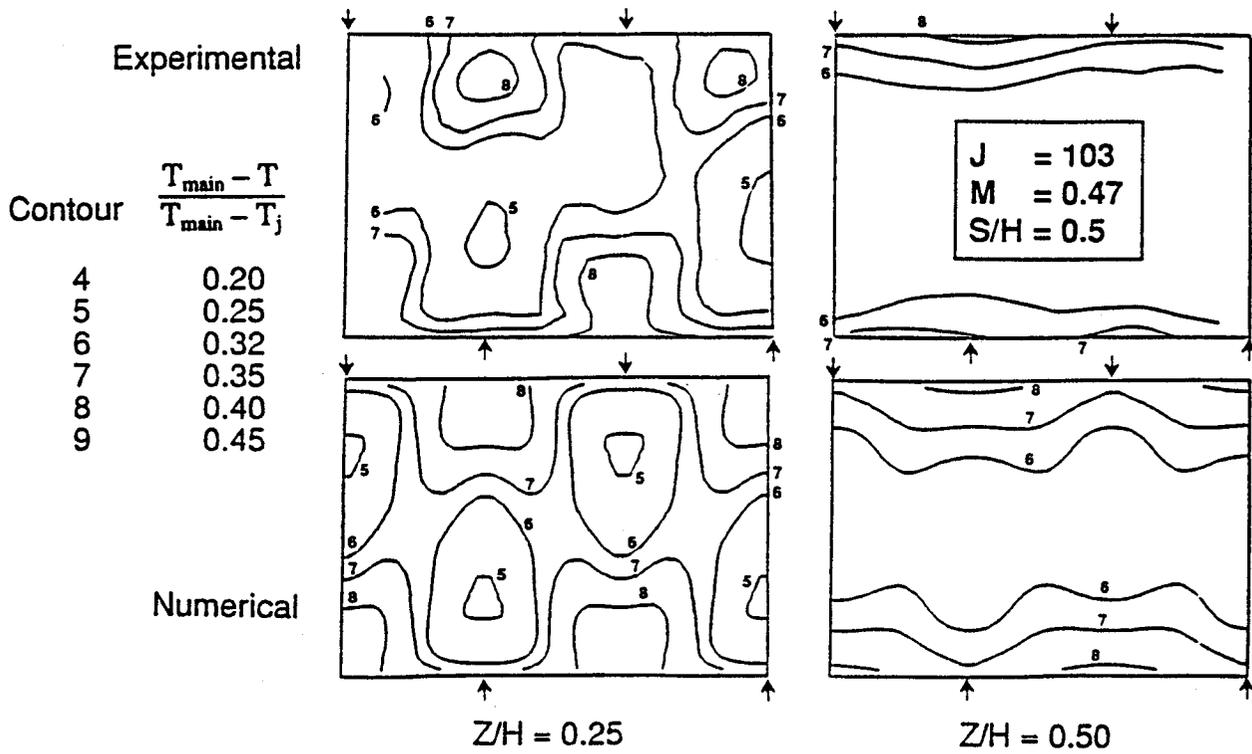
Figure 6. Comparison of Predicted and Measured Temperatures: Case 1

9

| Contour	$\dfrac{T_{main} - T}{T_{main} - T_j}$
1	0.05
2	0.10
3	0.15
4	0.20
5	0.25
6	0.33
7	0.35
8	0.40
9	0.45
10	0.50
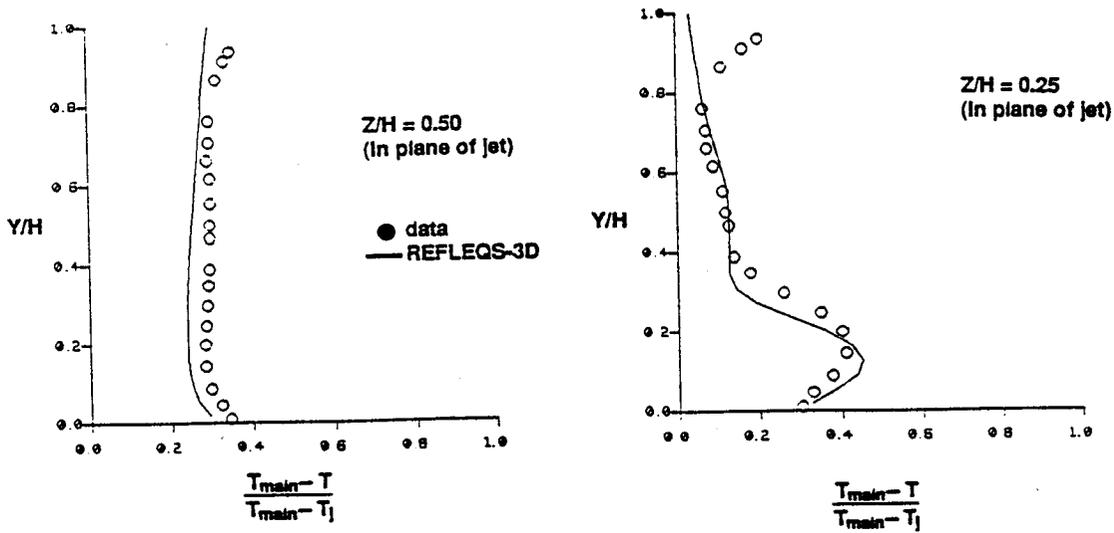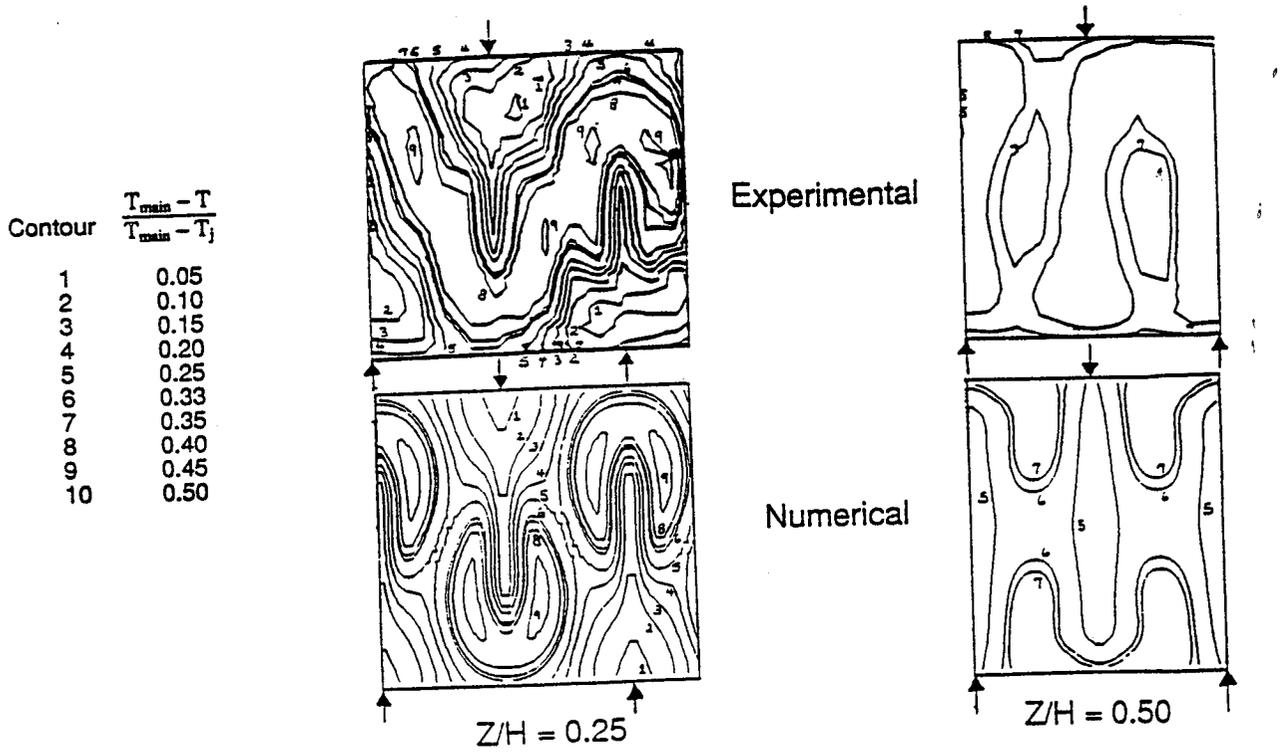
Figure 7. Comparison of Predicted and Measured Temperatures: Case 2

2. The preprocessor was modified to recognize a multitude of new species (*e.g.* OH, O, N, CO, H, *etc.*) required for this project. Since variable fluid properties were assumed in the numerical calculations, the variation of specific heats and viscosities were obtained for the above-mentioned species from Standard JANNAF tables, and coded into the preprocessor.

3. The specification of inlet velocity boundary conditions was modified. The code required the velocity at the inflow boundaries in terms of the contravariant components. The velocity components needed to be converted to contravariant components from cartesian components based on the local grid curvature data. Features facilitating use of cartesian components at external boundaries were implemented.

3.2   Combustion Heat Release Model

At the start of the project, only five species were available in REFLEQS for modeling chemical reactions: H_2, O_2, CO_2, H_2O, and C_nH_n. Additional species were added for this study, specifically OH, H, CO, and O. These species were needed to model the rich burn gases entering the mixer section, and for accurate modeling of stoichiometric temperatures as the dilution jets reacted.

Multi-step reactions can be modeled in REFLEQS by specifying reaction constants for each reaction step. However, after reviewing the time scales for heat release reactions at cruise-type conditions in RQL mixers, it was determined that reaction times were much faster than mixing times. Hence, the combustion process is mixing controlled, and instantaneous reaction rates were assumed.

3.3   NO$_x$ Model

The REFLEQS code was modified to model the formation of NO_x in the combustor. It was assumed that the NO_x reactions did not contribute to the overall heat release in the combustor, thus allowing the NO_x reactions to be "decoupled" from the aforementioned heat release reactions. NO_x was calculated as a passive scalar after the computation of the reacting flowfield.

A simple Zeldovich reaction scheme was used to model the NO_x formation. According to the mechanism, *NO* formation can be described by:

$$N_2 + O \leftrightarrow NO + N$$

and

$$O_2 + N \leftrightarrow NO + O.$$
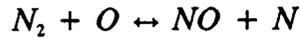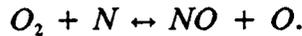
The first reaction is much slower than the second one and hence controls the rate of *NO* formation. If the concentration of *NO* is much smaller than the corresponding equilibrium value, the rate equation for *NO* can be written as:

$$\frac{d(NO)}{dt} = K[N_2][O]$$

Approximating the concentrations of N_2 and O by the local equilibrium values, the rate equation is given by

$$\frac{d(NO)}{dt} = A \exp\left(\frac{-E}{RT}\right) [N_2][O_2]^{1/2}$$

From Marble [15], the rate constants were determined to be:

$$A = 5.74 \times 10^4 \ \frac{1}{sec} \ \sqrt{\frac{moles}{m^3}}$$

$$\frac{E}{R} = 6.7 \times 10^{11°}K$$

In Phase II, a more complete model will be incorporated into the code. However, the basic NO_x mechanism should be captured with this simplistic one-step model.

After implementation into REFLEQS, the NO_x model was calibrated against the experimental results of Anderson [16], who used a premixed, prevaporized laboratory combustor. The REFLEQS test case consisted of premixed propane and air reacting in a straight channel. Instantaneous heat release was assumed. Marble's constants had to be modified to give good agreement with Anderson's data. The final constants used in this study were:

$$A = 3.3 \times 10^4 \, \frac{1}{sec} \, \sqrt{\frac{moles}{m^3}}$$

$$\frac{E}{R} = 1.03 \times 10^{14 \circ} K$$

Figure 8 shows the computed results compared to Anderson's data of Emission Index (EI) as a function of adiabatic flame temperature.
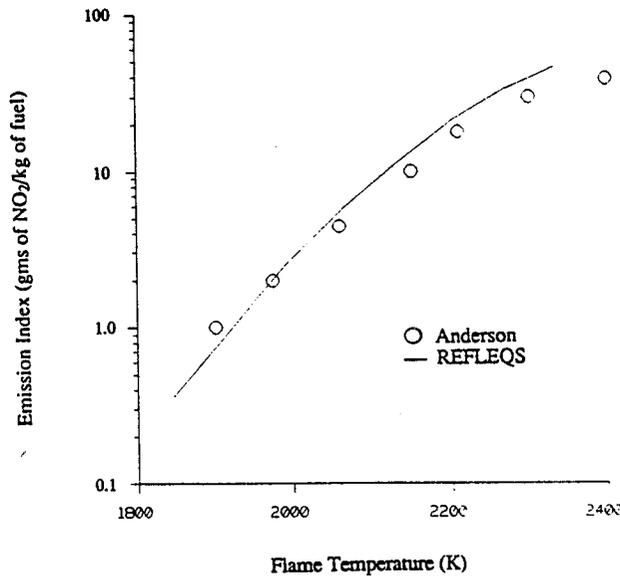

Figure 8. Calibration of NO_x Model in REFLEQS

3.4 Postprocessing

A number of modifications were required to process the numerical results for this study. These are described below.

Mixing Effectiveness. Temperature mixedness can be quantified in a number of different ways, including:

1. Pattern Factor (PF), defined as

$$PF = \frac{T_{max} - T_{avg}}{T_{avg} - T_{in}}$$

13

2. Standard Deviation (SD) defined as

$$SD = \frac{\sqrt{\dfrac{\sum_i \left(T_i - T_{avg}\right)^2}{n}}}{T_{avg}}$$

3. Mass-weighted Standard Deviation (MWSD), defined as

$$MWSD = \frac{\sqrt{\dfrac{\sum_i m_i \left(T_i - T_{avg}\right)^2}{\sum_i m_i}}}{T_{avg}}$$

4. Mass-weighted first absolute moment about the mean (FAM), defined as

$$FAM = \frac{\sum_i m_i \left|T_i - T_{avg}\right|}{\sum_i m_i \, T_{avg}}$$

MWSD and PF were selected for evaluating mixedness in this study. The lower the value of MWSD and PF, the better the mixing. The postprocessor was modified to calculate the value of MWSD and PF in various axial planes.

NO$_x$ Emission Index.   Tacina [2] has indicated that NO_2 emission index is a good way to quantify and compare NO$_x$ emissions from different configurations and test conditions. Even though the predominant NO$_x$ species in exhaust gases is NO, the emission index is defined in terms of gms of NO_2 per kg of fuel with the assumption that all the NO$_x$ eventually will be converted to NO_2 in the atmosphere.

In the one-step NO$_x$ model described earlier, NO is the predicted species that must be numerically converted to NO_2. This conversion is performed in the following manner in the preprocessor. From the reaction

$$2NO + O_2 \rightarrow 2NO_2,$$
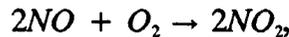
1.0 kg of NO would react with 0.53 kgs of O_2 to give 1.53 kgs of NO_2. Thus gms of NO was converted to gms of NO_2 by:

$$\text{gms of } NO = 1.53 \text{ gms of } NO_2$$

The *NO* concentrations at any axial plane were integrated to obtain the mass flow rate of *NO*. This value was multiplied by 1.53 and divided by the fuel mass flow of the combustor. Emission index is thus defined as gms of NO_2 generated per kg of fuel consumed.

Data Processing. Due to the geometric symmetry of the conventional mixer, only a part of the circular cross-section (pie section with central angle of 30 degrees) was considered for CFD analysis. For AJP configurations, half of the circular cross-section had to be modeled. For comparison of the two designs, it was deemed necessary to have similar geometrical domains. A simple FORTRAN code was used to postprocess the numerical results from the conventional mixer to the same computational domain as the AJP configurations.

4. ANALYSIS OF CONVENTIONAL MIXER DESIGN

A conventional mixer design was studied first. An *optimized* conventional configuration was desired for an objective comparison to the AJP mixer concept. A geometry compatible with the NASA LeRC flametube combustor was selected as described below, and analyses were performed at various jet momentum flux ratios to determine the "best" baseline case. Both reacting and non-reacting cases were analyzed. The geometry, numerical grid, numerical details, boundary conditions, grid independence, convergence criteria, and results are discussed below.

4.1 Geometry

In order to make the Phase I study applicable to the NASA LeRC flametube combustor, the quick-mix geometry was mimicked in the CFD analysis. The geometry of the conventional mixer design consisted of three components: an inlet pipe, converging section and the quick-mix section (see Figure 9). The inlet pipe was six inches (0.152m) - in diameter and three inches (0.076m) in length. The inlet pipe converged into the quick-mix section which was five inches (0.127m) in diameter. The length of the quick-mix section was thirteen inches (0.333m).

There were twelve slots located symmetrically around the perimeter of the quick-mix section. The axial location of the slot centerline was three inches (0.076m) from the inlet

of the quick-mix section. The slots were rectangular in shape with an aspect ratio of four and aligned in the streamwise direction. Rectangular slots were chosen because of their simplistic design and ease of modeling. Slanted slots were not considered for analysis in Phase I because the whole 360 degree cross-section would have to be modeled, thus reducing grid resolution. The analysis of quick-mix sections with slanted slots will be performed in Phase II of this project.
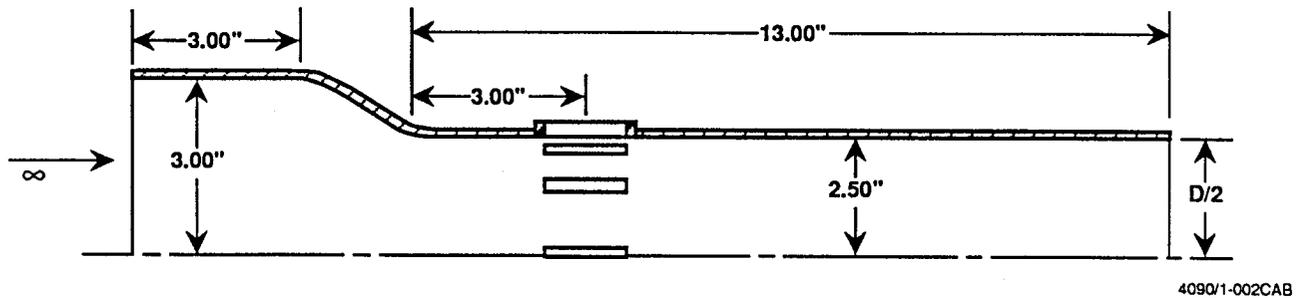

Figure 9. Schematic of Conventional Quick-Mix Geometry Modeled in
This Project

Due to geometric symmetry, only one slot was modeled with planes of symmetry set up halfway between adjacent slots. This allowed greater grid resolution and reduction of computer turnaround time. This reduced the rɵ domain to a pie section with the central angle of thirty degrees.

4.2   Grid

During the early stages of the project, a number of coarse grids were employed to study the flow and optimize the convergence characteristics of the quick-mix section. A baseline grid of 9,216 cells (32x16x18 in x,r,ɵ directions) was finally selected and used for modeling the conventional mixer. The grid is shown in Figure 10. The axial grid spacing is dense near the slot, and gets coarser upstream and downstream of the slot. The grid in the radial direction was non-uniform with greater density near the combustor wall. The grid in the transverse direction was uniform in the slot, and slowly expanding away from the slot. The slot was represented by 6x6 mesh. As will be discussed in grid independent studies, this rather coarse grid is not grid-independent, but it does capture all of the relevant flow features. For comparative studies, it was felt sufficient.

Figure 10. Grid Used for Conventional Mixer

GRID: x = 32
r = 16
θ = 18

Section A-A

Transverse Boundary

Transverse Boundary

JET

θ

JET

x

r

A

A

17
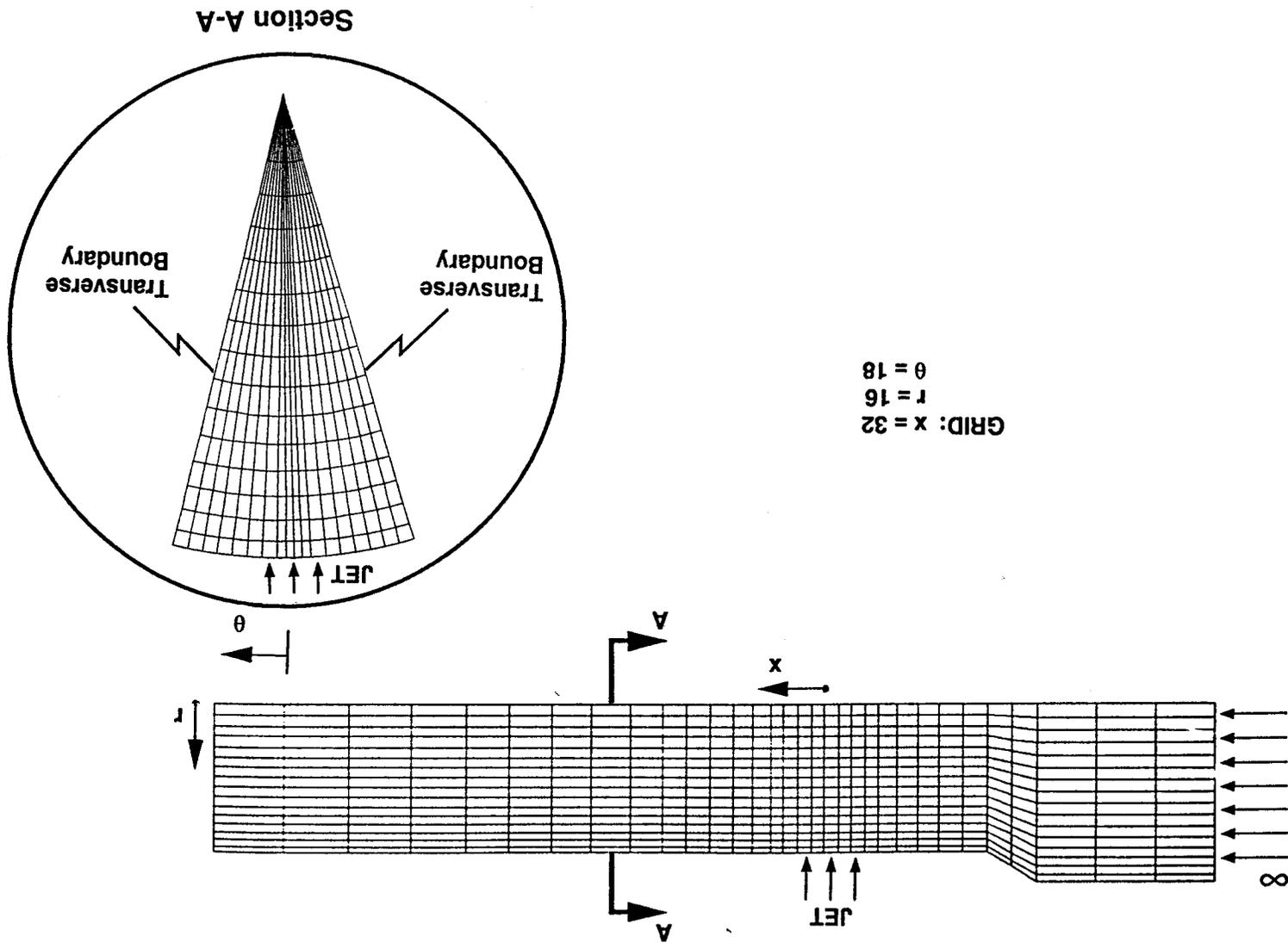
4.3 Numerical Details

The REFLEQS code with appropriate modifications stated earlier was used for this project. The numerical details of the calculations included:

1. Whole field solution of u-momentum, v-momentum, w-momentum, pressure correction, turbulent kinetic energy k, dissipation rate ϵ, total enthalpy, and mixture fraction;
2. Upwind Differencing;
3. Variable Fluid Properties (*i.e.* temperature dependency of specific heat, laminar viscosity, *etc.*);
4. Adiabatic Walls;
5. Standard k-ϵ Model with wall functions;
6. Instantaneous heat-release model; and
7. Nine chemical species.

4.4 Boundary Conditions

Mainstream Boundary. At the mainstream inlet boundary, propane and air are assumed to have completely reacted at an equivalence ratio of 1.6. The species and temperature of the reaction products were taken from the JANNAF-standard rocket code named One Dimensional Equilibrium (ODE) [17]. Velocity and pressure were obtained from experimental test plans for the RQL flametube combustor [18]. A uniform velocity profile was assumed with turbulence typical of primary zones in gas turbine combustors. The mainstream inlet conditions were:

Axial velocity	=	35.5 m/s
Temperature	=	2221°K
Density	=	2.0 kg/m^3
Composition (mass fraction)	=	0.134 CO, 0.068 CO$_2$, 0.006 H$_2$, 0.096 H$_2$O, 0.696 N$_2$
Turbulent intensity (u'/U)	=	50%
Turbulent length scale (l/D)	=	0.02

18

Jet Inlet. The composition at the dilution jet inlet was assumed to be air. A uniform velocity profile was assumed, along with the following conditions:

Mass flux ratio (m_j/m_∞)	=	1.94
Jet temperature	=	811°K
Density	=	6.35 kg/m^3
Composition (mass fraction)	=	0.232 O_2, 0.768 N_2
Turbulent intensity (v'/V)	=	10%
Turbulent length scale (l_j/D)	=	0.13

The jet momentum flux ratio (J) was varied parametrically from 16 to 64. The corresponding radial velocities varied from 120 m/s to 240 m/s. For each J, the slot flow area was modified to maintain constant jet flow.

Exit Boundary. The exit boundary condition was a zero gradient boundary condition. All variables were extrapolated to the exit from the interior.

Transverse Boundaries. The transverse boundaries in Figure 10 were assumed to be slip walls with no flow leaving the domain across them. These boundaries were also tested for outflow by setting them to be periodic boundaries (meaning properties leaving one cell on one boundary enter the corresponding cell on the other boundary).

Combustor Wall. The combustor wall was treated as a no-slip adiabatic wall (zero enthalpy gradient). Wall functions were used for the turbulent quantities (k and ϵ).

Centerline. The computational boundary at the centerline was assumed to be a symmetry plane.

4.5 Grid Independence

Two different sizes of grids were run to test grid independence: 9,216 and 52,650 cells. The finer grid was obtained by increasing the grid density by ~75% in all three directions. Most of the increased grid cells in the axial direction were concentrated in the vicinity of the slot and downstream of the slot. In the radial direction, the same grid stretching was

employed. In the θ direction, the grid was more densely packed to the center of the domain near the jet. Comparison of the two grids is shown in the Figure 11.

Computational results from the two grids are presented in Figure 12 for a momentum flux ratio (J) of 32.0. The isotherms in an rx plane through the jet centerline are shown and compared in Figure 12. Qualitatively they exhibit similar features. The jet seems to have penetrated a little further in the case of the fine grid. Isotherms are also shown for two axial planes downstream of the jets: x/D = 0.0 and 2.0. The isotherms at x/D = 2.0 show slightly higher temperatures (~22°K) for the fine grid. Also, the cold region in the fine grid solution is located closer to the centerline, indicating greater penetration. However, overall the coarse grid solution is very similar to the fine grid solution.

The highest momentum flux case (J = 64) exhibited jet backflow toward the rich burn section. Figure 13 shows the results for the two grids. As seen in Figure 13, the regime of backflow looks identical in size in both the cases. Overall agreement is better than for the J = 32 case.

Based on this grid-independence study, it appears the coarse grid captures the overall physics of the problem, and can be used to qualitatively compare quick-mix designs.

4.6   Selection of Transverse Boundaries

Due to reported asymmetric flow features in geometrically symmetric geometries [19], it was considered important to check the symmetric transverse boundary assumption used in this study. Figure 14 shows results in terms of isotherms for the J = 32 case with periodic boundaries as compared to symmetric transverse boundaries. The isotherms are essentially identical in the planes shown. Thus the symmetric transverse boundaries are adequate for modeling conventional slotted holes.

4.7   Convergence Criteria

The summation of all error residuals were reduced five orders of magnitude, and continuity was conserved in each axial plane. Typically, convergence required approximately 150 iterations as shown in the Figure 15. The relaxation on the velocity components (u and v only) was continuously varied during the run through a user specified

Section A-A

A

A

GRID: x = 32   **9216 CELLS**
r = 16
θ = 18

B

B

GRID: x = 60   **52,650 CELLS**
r = 30
θ = 27
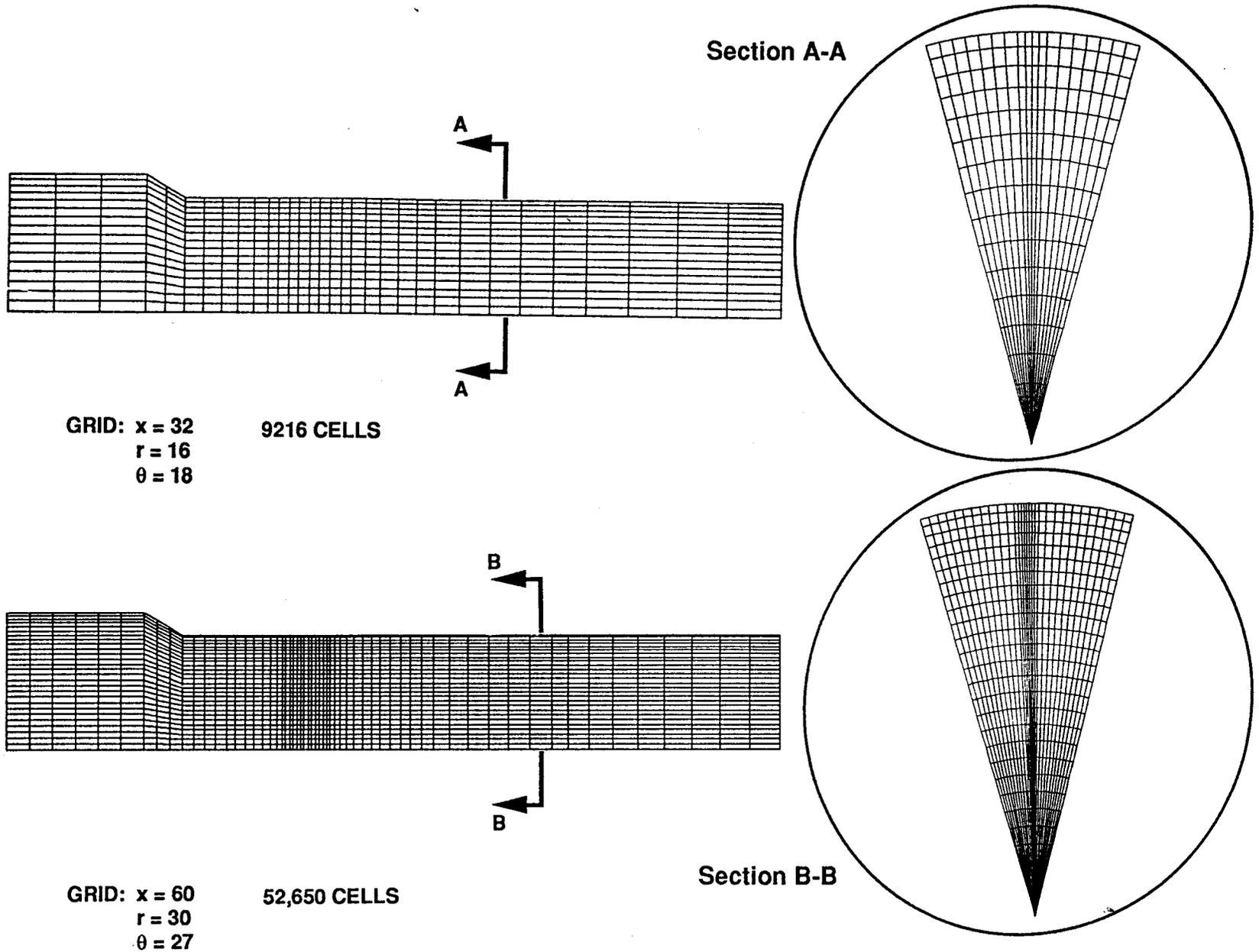
Section B-B

Figure 11. Comparison of Coarse and Fine Grids for Conventional Mixer

COARSE

FINE

a) rx plane: slot C_L

Section A-A
x/D=0.0

CONTOUR LEVELS	
1	800
2	850
3	900
4	950
5	1000
6	1050
7	1100
8	1150
9	1200
10	1250
11	1300
12	1350
13	1400
14	1450
15	1500
16	1550
17	1600
18	1650
.	.
31	2300

Section B-B
x/D=2.0

b) rθ planes
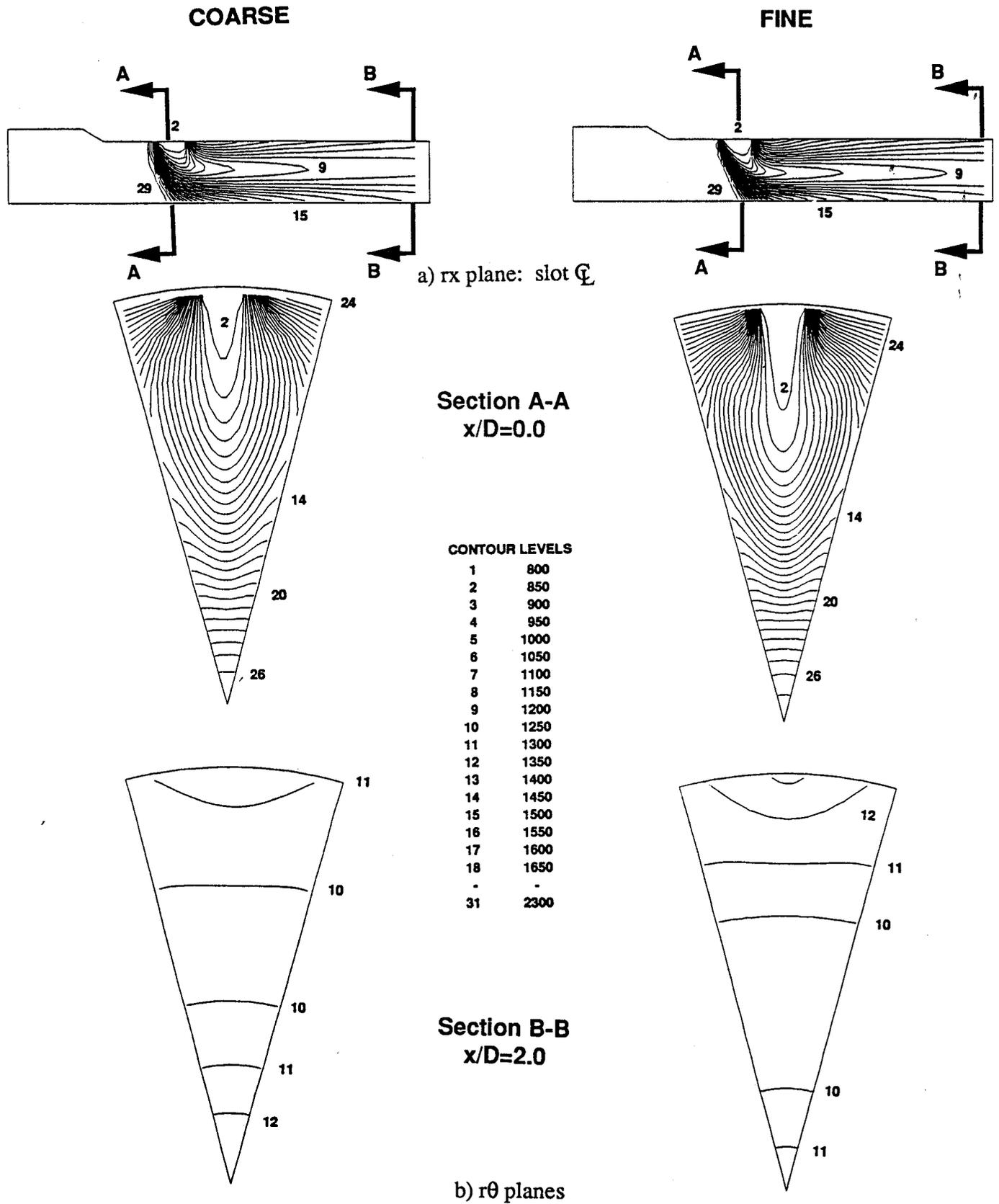
Figure 12. Isotherms for Conventional Mixer Using
Coarse and Fine Grids: J=32
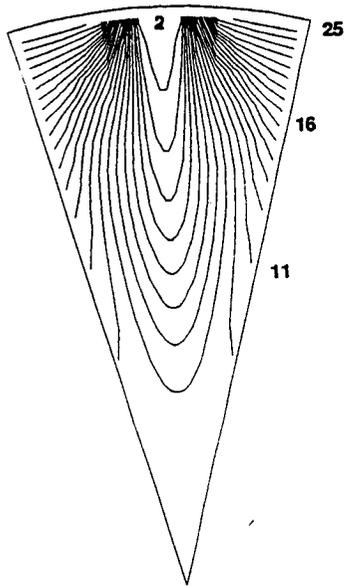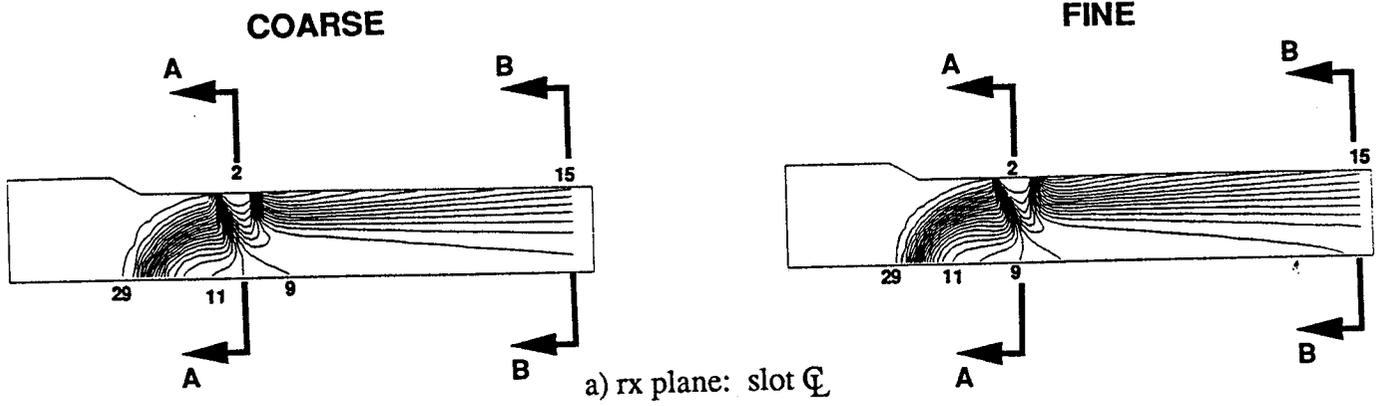
COARSE

FINE

a) rx plane: slot C_L

Section A-A
x/D=0.0

CONTOUR LEVELS

1	800
3	900
5	1000
7	1100
9	1200
11	1300
13	1400
15	1500
17	1600
19	1700
21	1800
23	1900
25	2000
27	2100
29	2200
31	2300
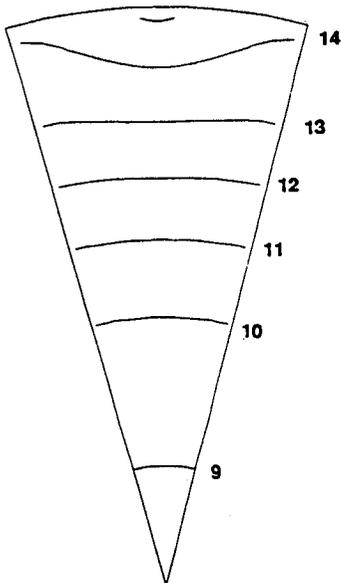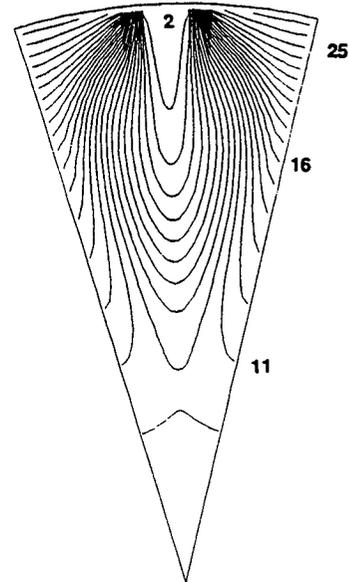
Section B-B
x/D=2.0
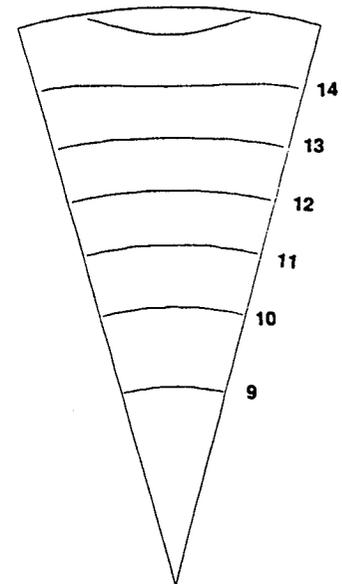
b) rθ planes

Figure 13. Isotherms for Conventional Mixer Using
Coarse and Fine Grids: J=64

23

SYMMETRIC

PERIODIC

a) rx plane: slot C_L

Section A-A
x/D=0.0

CONTOUR LEVELS	
1	800
3	900
5	1000
7	1100
9	1200
11	1300
13	1400
15	1500
17	1600
19	1700
21	1800
23	1900
25	2000
27	2100
29	2200
31	2300

Section B-B
x/D=2.0

b) rθ planes
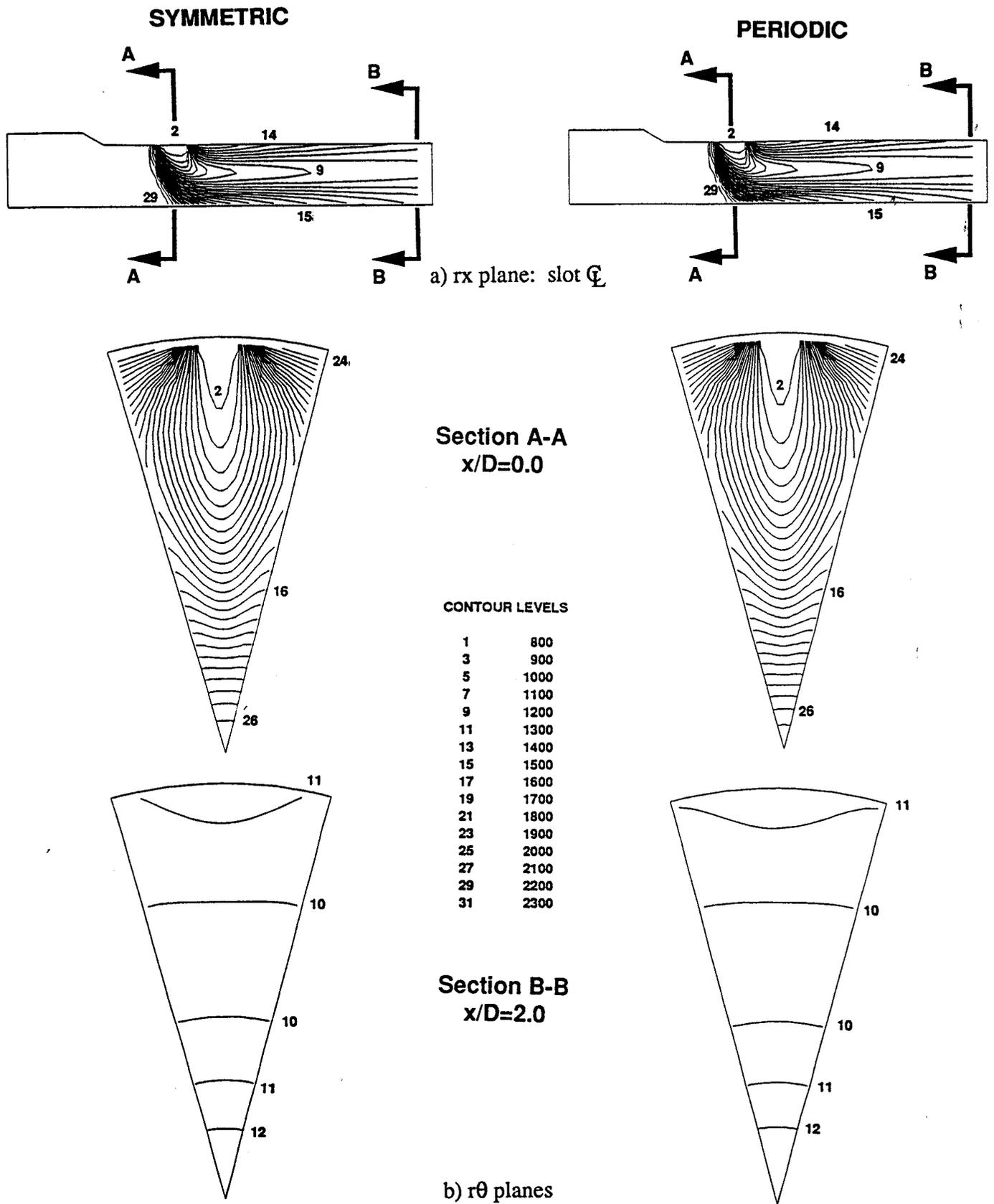
Figure 14. Isotherms for Conventional Mixer Using Symmetric and Periodic Transverse Boundaries: J=32
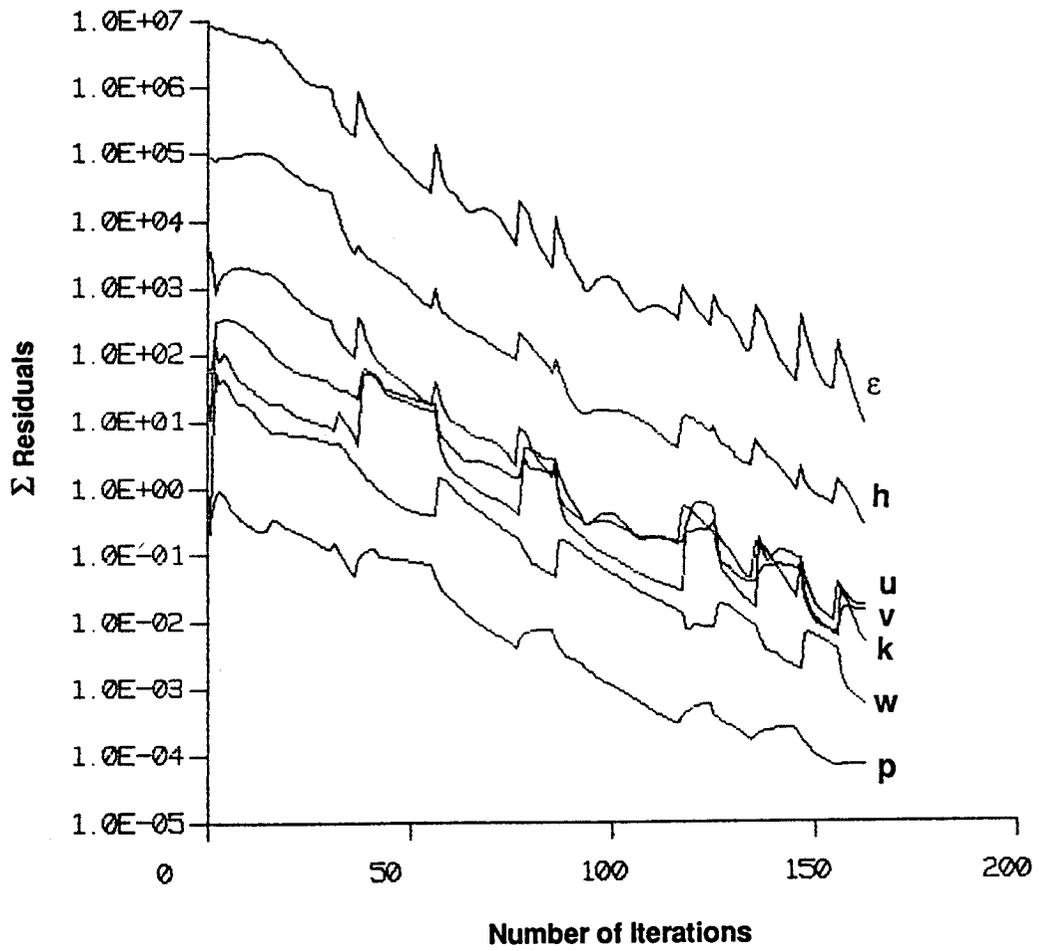
Figure 15. Convergence History for a Typical Run

input file. The repeated variation of relaxation allowed resolution of different scales of numerical error. This was found to speed up convergence by a factor of four compared to constant relaxation. Approximately 3 CPU hours were required on an Alliant FX/8 mini-supercomputer. Fine grid calculations took approximately 500 iterations and 40 CPU hours. For comparison, the ALLIANT computer speeds are ~20 times slower than a CRAY X-MP.

4.8   Results

Parametric numerical tests were performed for various jet momentum flux ratios, and for non-reacting and reacting gases. Discussion of the findings are reported below. Graphical predictions of all cases are provided in Appendix A in color.

Typical Flow Features.   One of the most striking physical features of a dilution jet injected normally into the mainstream is the appearance of vortex roll up downstream of the jet injection [20]. Figure 16 shows velocity vectors for the $J = 32$ case for different axial locations downstream of the jet corresponding to $x/D = 0.0, 0.3, 0.5, 1.0$ and 2.0. The vortex roll up is clearly visible. Figure 17 shows isotherms at the same axial locations as the previous figure. The isotherms show the location of the center of jet stream occurring at approximately mid-radius.

Non-Reacting Flows.   In an effort to find the optimum conventional mixer, the jet momentum flux ratio was parametrically varied. Five momentum flux ratios were tested: 16, 32, 40, 48, and 64. All other flow conditions were held constant, including mass flow ratio (jet-to-mainstream) at 1.94. To maintain a constant mass flow, the slot size was changed for each J. The slot aspect ratio was held constant at four, and was always centered at the same location. The same number of grid cells were used in all the cases. However, since the slot size was changing, the grid density had to be slightly altered for each case. This variation is thought to have a minimal effect on the results discussed below.

The computed results were examined at two axial planes downstream of the jet inlet: $x/D = 1.0$ and $x/D = 2.0$. Figure 18 shows the isotherms at $x/D = 1.0$ and Figure 19 shows the isotherms at $x/D = 2.0$. The radial location of the lowest temperatures indicates the penetration location of the cold jet. As expected, increased jet penetration can be seen

x/D=0.0

Max. Velocity =175.0 m/s

x/D=0.3

91.0 m/s

x/D=0.5

14.0 m/s

x/D=1.0

3.3 m/s

x/D=2.0

0.7 m/s
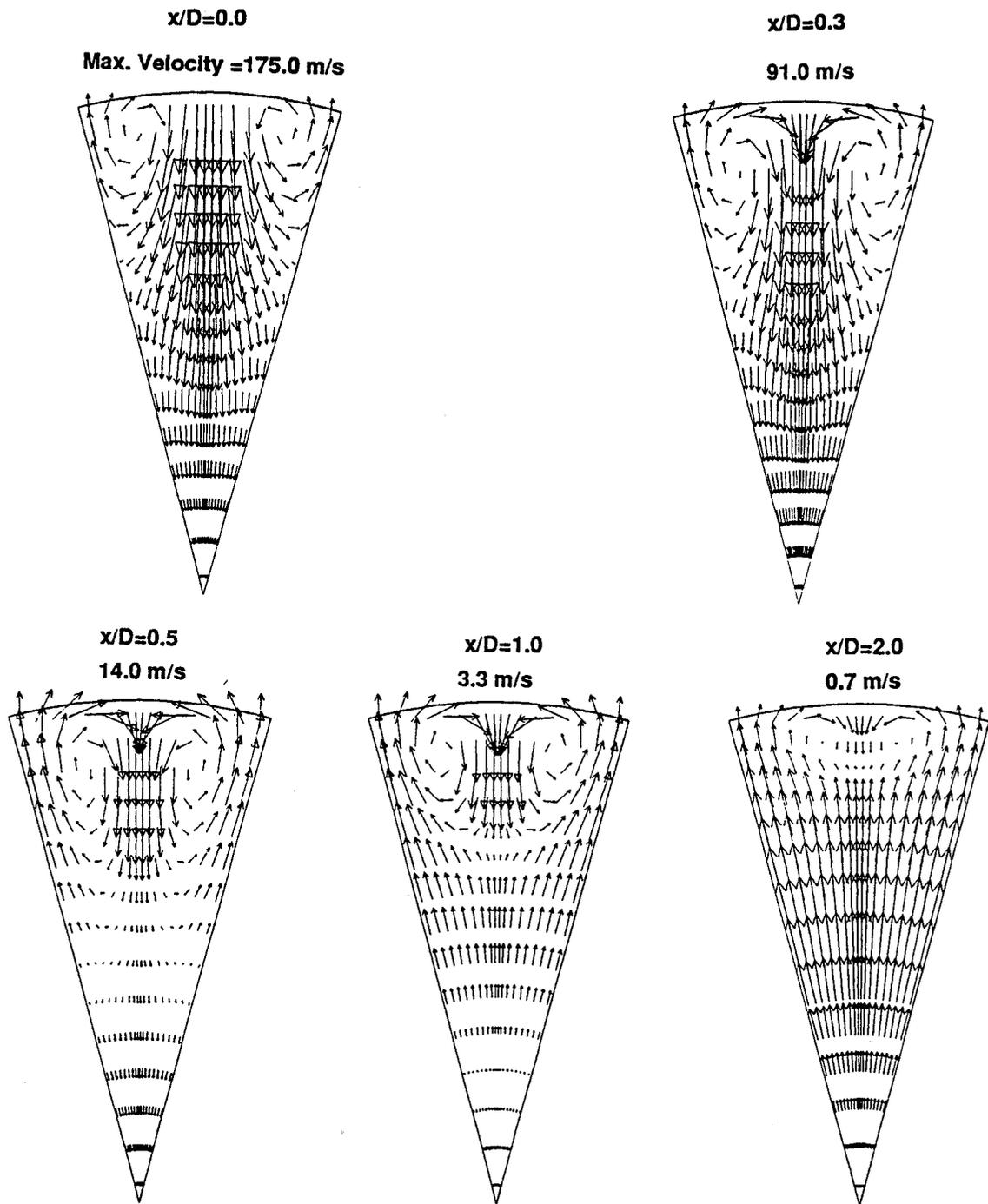
Figure 16. Flow Patterns of Conventional Mixer: J=32
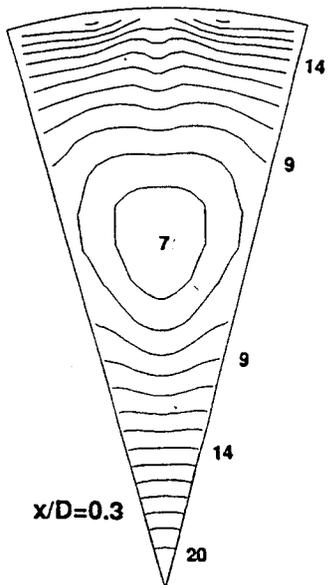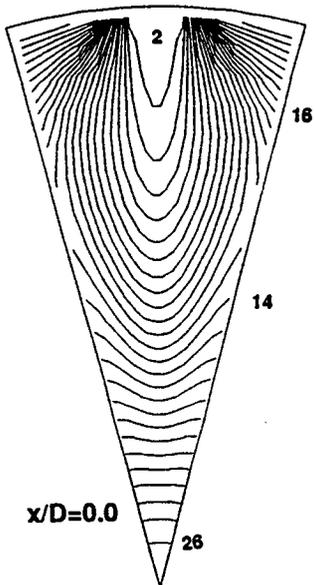
27

CONTOUR LEVELS

1	800
3	900
5	1000
7	1100
9	1200
11	1300
13	1400
15	1500
17	1600
19	1700
21	1800
23	1900
25	2000
27	2100
29	2200
31	2300
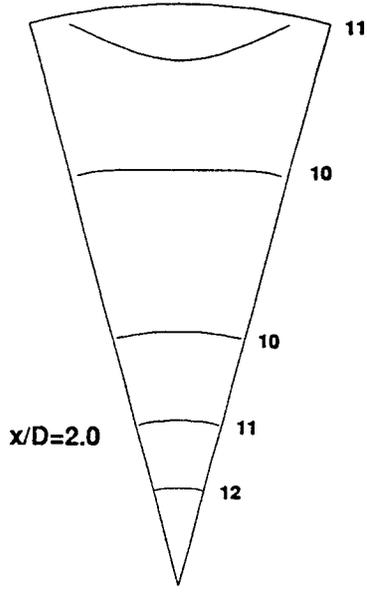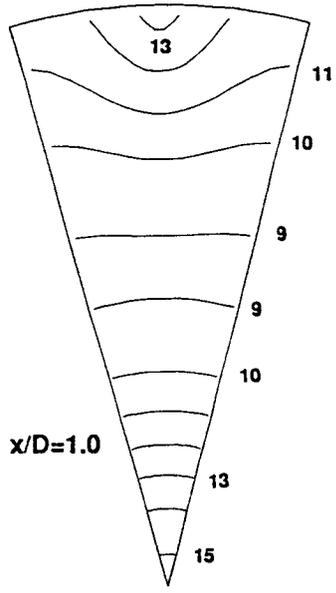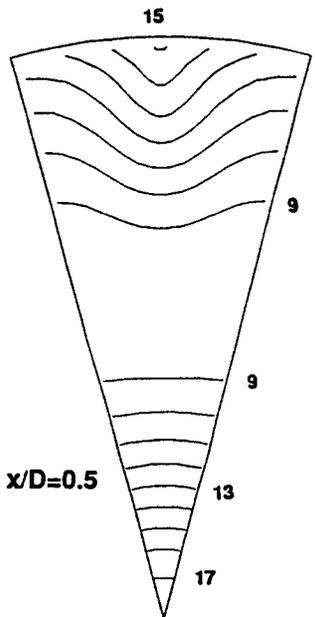
Figure 17. Isotherms of a Conventional Mixer: J=32

J = 16

J = 32

12

13

10   10   24

11   9 9   12   15

J = 40

CONTOUR LEVELS

1	800
3	900
5	1000
7	1100
9	1200
11	1300
13	1400
15	1500
17	1600
19	1700
21	1800
23	1900
25	2000
27	2100
29	2200
31	2300

14

11

12   10   10

J = 48

J = 64

16

17

14   12   10   10

14   12   10   9
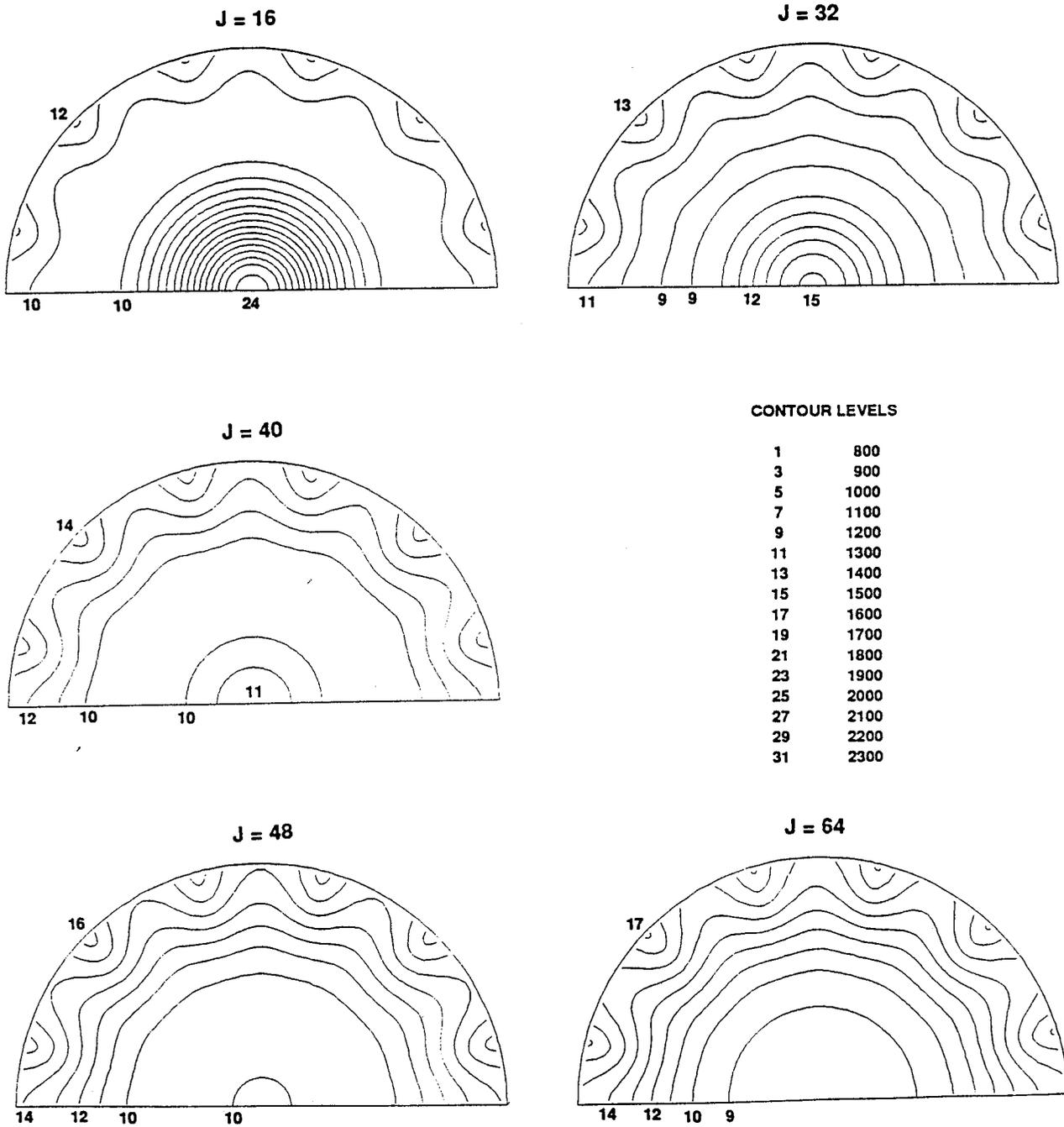
Figure 18. Isotherms of Conventional Mixer for Non-Reacting
Conditions: x/D=1.0

29
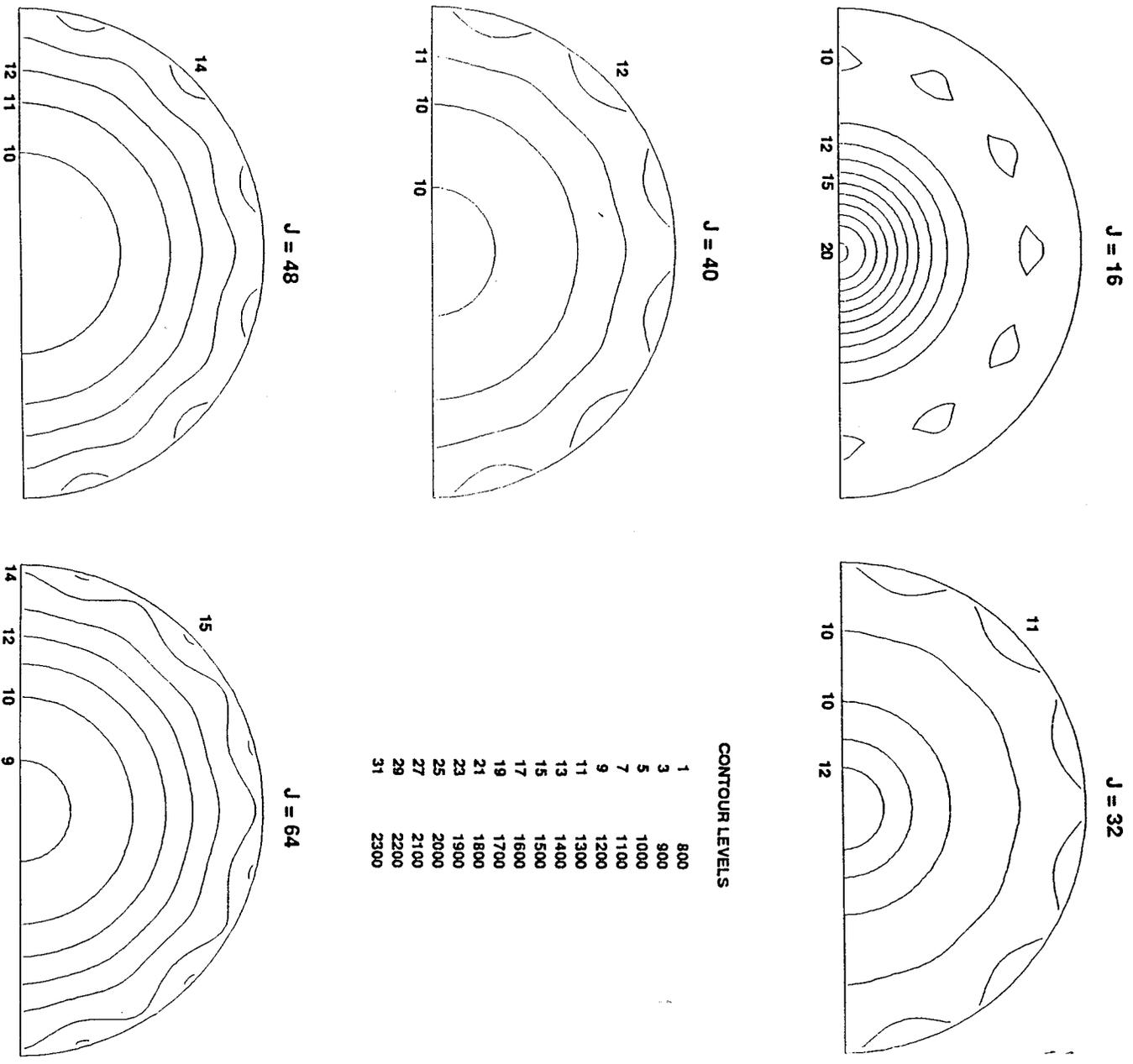
Figure 19. Isotherms of Conventional Mixer for Non-Reacting
Conditions: x/D=2.0

30

for larger values of J. The temperature spread between maximum and minimum temperatures is an indicator of the mixing effectiveness of each case. The best mixing results were obtained when the jet penetrates to approximately mid-radius. J = 32 and 40 appear to be near optimum mixers.

A more quantitative comparison of the non-reacting mixing effectiveness is shown in Figure 20. In Figure 20, the MWSD of temperature is presented versus J. It can be seen that J = 32 and J = 40 both have nearly equivalent mixing characteristics (0.043 and 0.051, respectively). Under-penetration is worse than over-penetration for the non-reacting mixers.
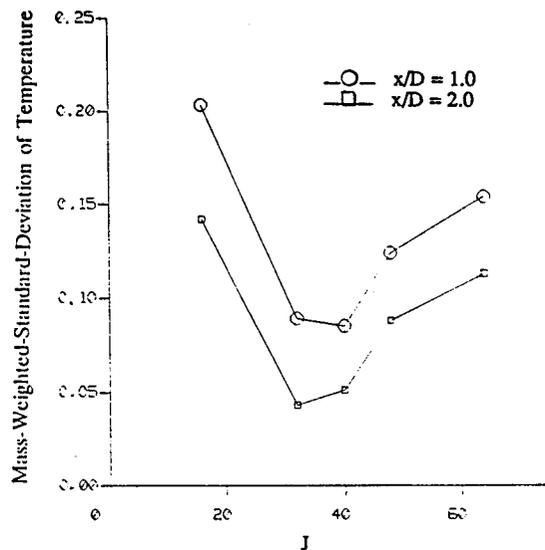

Figure 20. Mixing Effectiveness of Conventional
Mixer: Non-Reacting Flow

Reacting Flows.   The same cases were analyzed as discussed above, except chemical reaction was turned on. Due to reaction, the overall average temperature increased from 1219°K for non-reacting flows to 1789°K for reacting flows. Figure 21 shows isotherms for the reacting cases one diameter downstream of the jet center, while Figure 22 shows isotherms at a cross section two diameters downstream of the jet inlet. From these two figures (from comparing min-to-max temperature differences), it can be seen that J = 40 seems to be the best mixer. This can be further elucidated by looking at the mixing effectiveness (defined as MWSD of temperature) shown in Figure 23. Figure 23 clearly shows J = 40 to be the best mixer (MWSD = 0.076 at x/D = 2.0). J = 32 can no longer claim this honor (MWSD = 0.102).

31

J = 16

J = 32

11

10 9 9 12 17 17 19

13

10 9 9 18

J = 40

14

10 9 9 14 10

CONTOUR LEVELS

1	800
2	900
3	1000
4	1100
5	1200
6	1300
7	1400
8	1500
9	1600
10	1700
11	1800
12	1900
13	2000
14	2100
15	2200
16	2300
17	2400
18	2500
19	2600
20	2700

J = 48

16

12 10 9 10 11

J = 64

17

14 12 10 9
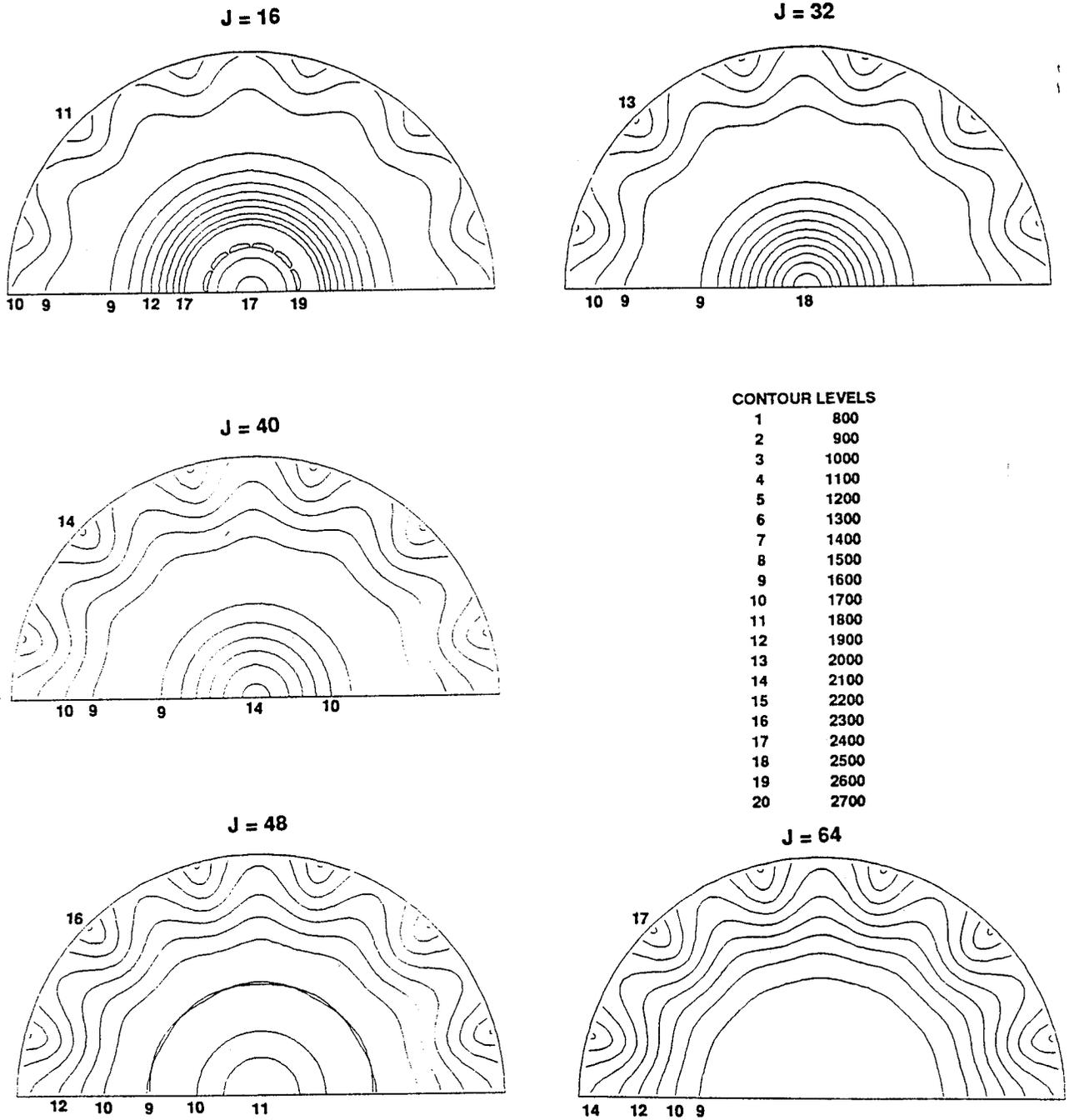
Figure 21. Isotherms of Conventional Mixer for Reacting
Conditions: x/D=1.0
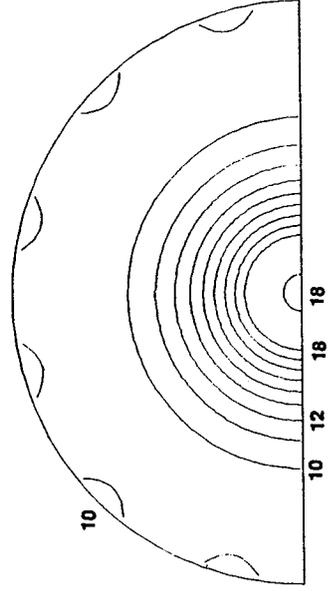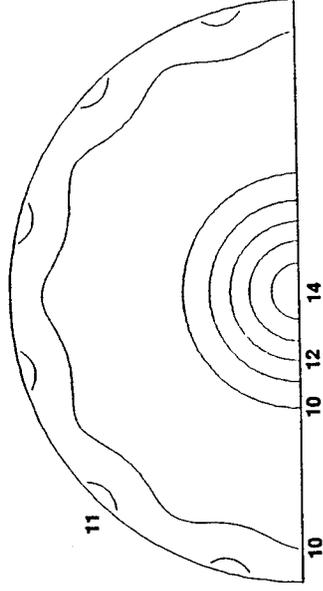
32

J = 32

J = 16

J = 40

J = 48

J = 64

CONTOUR LEVELS	
1	800
2	900
3	1000
4	1100
5	1200
6	1300
7	1400
8	1500
9	1600
10	1700
11	1800
12	1900
13	2000
14	2100
15	2200
16	2300
17	2400
18	2500
19	2600
20	2700
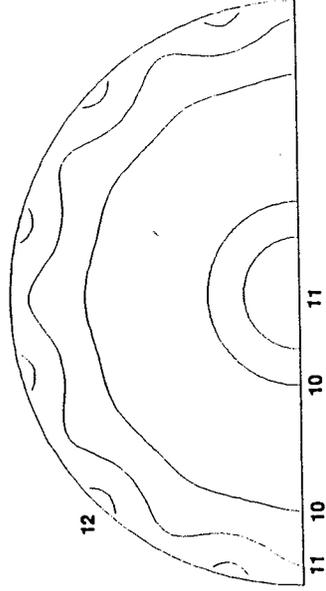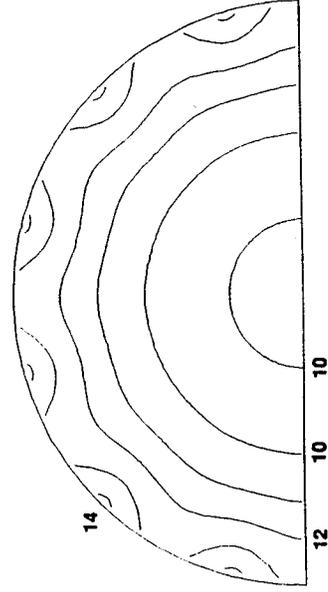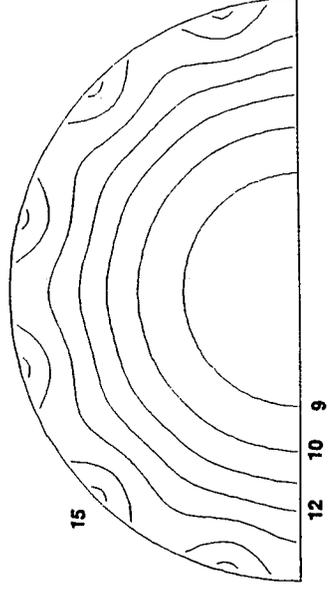
Figure 22. Isotherms of Conventional Mixer for Reacting
Conditions: x/D=2.0

33
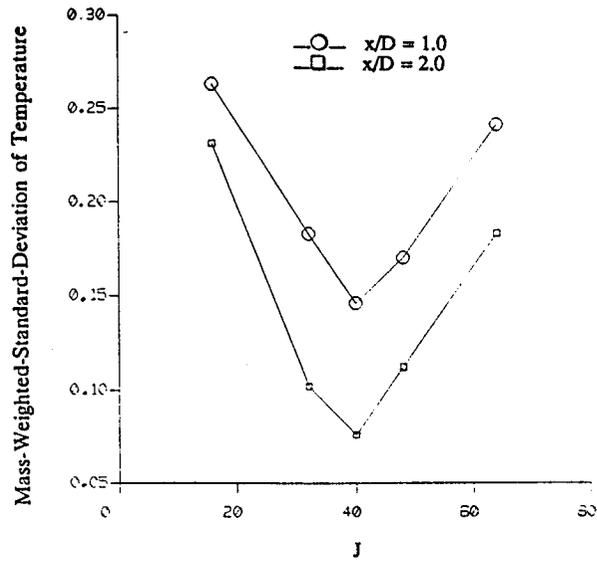
Figure 23. Mixing Effectiveness of Conventional
Mixer: Reacting Flow

In addition to mixing effectiveness, another important criteria for evaluation of quick-mix sections is combustion efficiency. In particular, CO concentrations should be essentially eliminated from the combustor exit. The CO emission level in various axial planes downstream of the dilution jet is displayed in Figure 24. For all cases except $J = 16$, it can be seen that the CO species has been oxidized (to CO_2) by $x/D = 0.25$. For $J = 16$, unreacted CO remains in the flowfield even at $x/D = 2.0$.
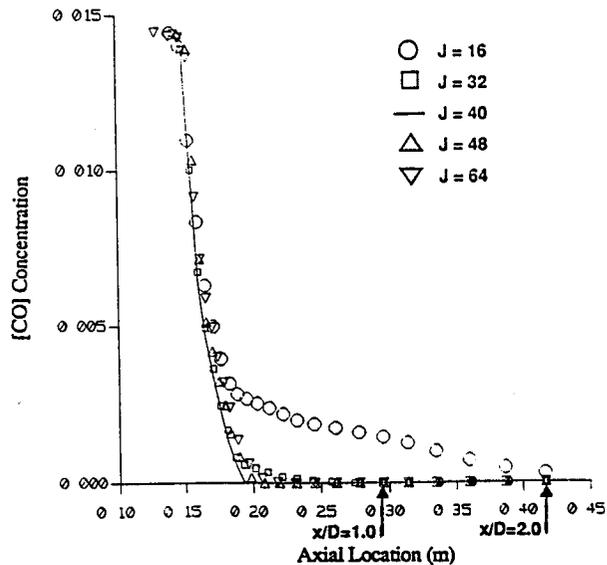
Figure 24. CO Emissions in Conventional Mixer

<u>NO_x Concentrations</u>.   NO$_x$ is most rapidly formed in high temperature regions when excess oxygen is available. Such zones occur in the shear layers between the dilution jet and the main stream. Reducing the size and duration of these high temperature regions substantially reduces NO$_x$ formation.

The NO$_x$ results are presented in terms of Emission Index (EI) and NO$_x$ ppm. For the optimum J = 40 case, EI = 2.81 at x/D = 1.0 and 2.87 at x/D = 2.0. Figure 25 shows the EI for different J values at two axial locations (x/D = 1.0 and 2.0). The difference in the value of EI at two locations indicates that NO$_x$ continues to form as the flow proceeds downstream. Alternatively, this difference says that mixing was not optimum. For the case of J = 40, hardly any change in the value of the EI is observed. At x/D = 1.0, EI = 2.81 while at x/D = 2.0, EI = 2.87. For the cases where J is away from the optimum, the EI varies by as much as 3.0 (J = 16). Figure 26 shows NO$_x$ emissions (ppm) for the two downstream locations. The worst J case is the highest J case (J = 64) due to jet backflow into the mainstream.

Figure 27 shows NO$_x$ concentrations convected out of each axial plane downstream of the jet inlet. Except for J = 16, all the cases show very little NO$_x$ formation downstream of x/D = 1.0. This indicates that high temperature zones are no longer existent. For the J = 16 case, NO$_x$ formation is increasing significantly downstream of x/D = 1.0, indicating high temperature and chemical reaction is still taking place.

<u>Comparison of Non-Reacting and Reacting Flow Results</u>.   The non-reacting tests show that J = 32 and J = 40 are the best mixers, and J = 16 has the worst mixing characteristics. The J = 64 case is a better mixer than J = 16 because of jet backflow into the mainstream. The reaction cases show that J = 40 is the best case with minimum emissions. The worst case is at J = 64, caused by jet backflow. Hence, what is advantageous for non-reacting mixedness, is detrimental for NO$_x$ emissions.

5.   ANALYSIS Of AJP CONCEPT

The Asymmetric Jet Penetration (AJP) concept was proposed for improved mixing characteristics and low NO$_x$ formation in the quick-mix section of the RQL combustor. The AJP concept strives to produce large scale mixing instead of small scale mixing characteristic of conventional, radial-inflow slots. This is accomplished by jet penetration
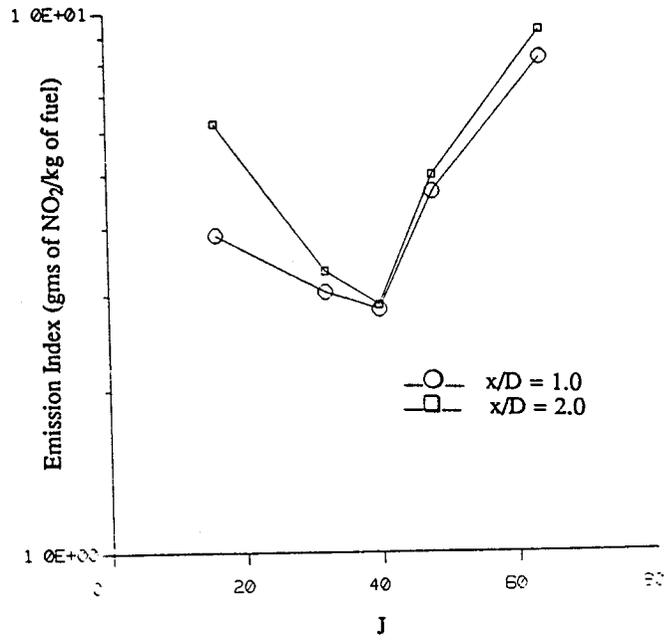
Figure 25. NO$_x$ Emission Index of Conventional Mixer
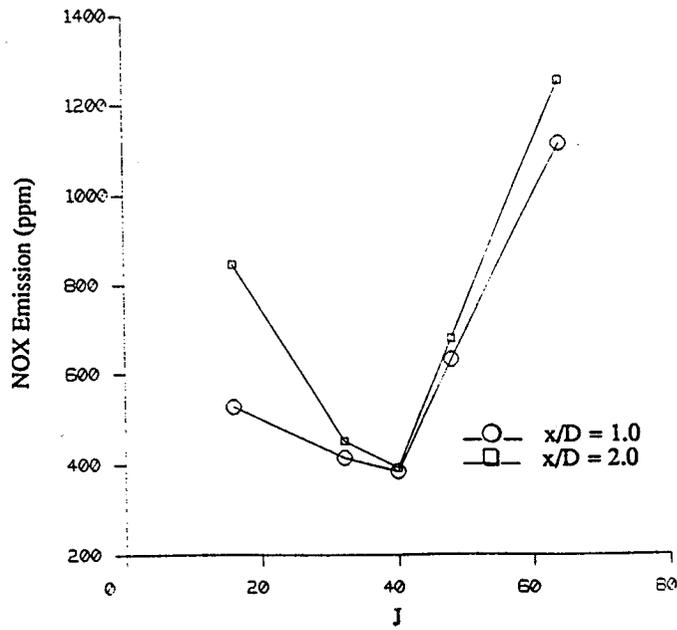
Figure 26. NO$_x$ Emissions (ppm) of Conventional Mixer

36

across the mainstream to the opposite wall. Figures 3 and 4 compare the generic differences between conventional and AJP designs.
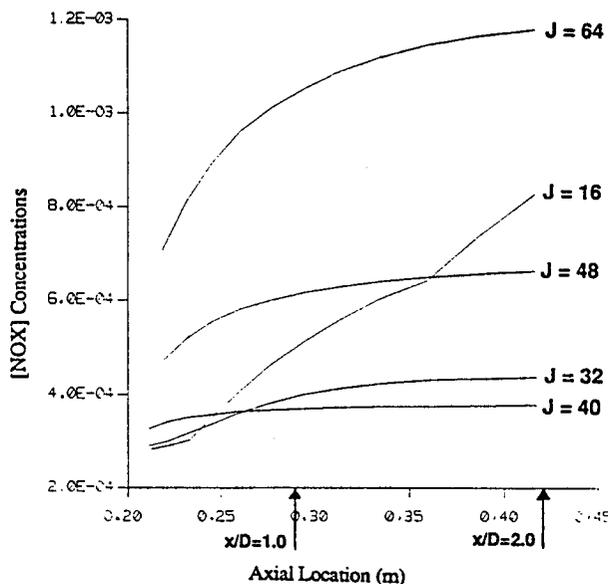

Figure 27. Formation of NO_x Downstream of the Dilution Jets

In many ways, the AJP concept is similar to staggered dilution holes in annular combustors, and the conventional design is similar to inline holes. In annular combustors, staggered jets have been shown to be superior to inline jets [19], especially if the jets penetrate to the opposite wall. Parameters which have a strong influence on mixing effectiveness in staggered hole arrangements include jet spacing-to-duct height and jet-to-mainstream momentum flux ratio.

Figure 28 from [19] shows the results of a CFD analysis of staggered dilution holes in a generic annular gas turbine combustor. In Figure 28, the mixedness (expressed as temperature pattern factor) is highly sensitive to spacing-to-duct height (S/H) ratio. The optimum spacing results in dramatic mixing improvements. Such improved mixing characteristics may also be achieved in can-type geometries with the AJP concept. Because mixing effectiveness is highly sensitive to jet spacing, it is highly unlikely that an optimum AJP configuration was found in this Phase I effort. However, two configurations were tested as discussed below. Additional analysis is necessary to fully evaluate the AJP concept.

37

$$PF = \frac{T_{max} - 1895°K}{1895°K - 811°K}$$

■ BASE TURBULENCE
● HIGH TURBULENCE

PF at 1.0H Downstream of Jets

J = 110
M = 0.5

S/H

Optimum from Holdeman *et al.*
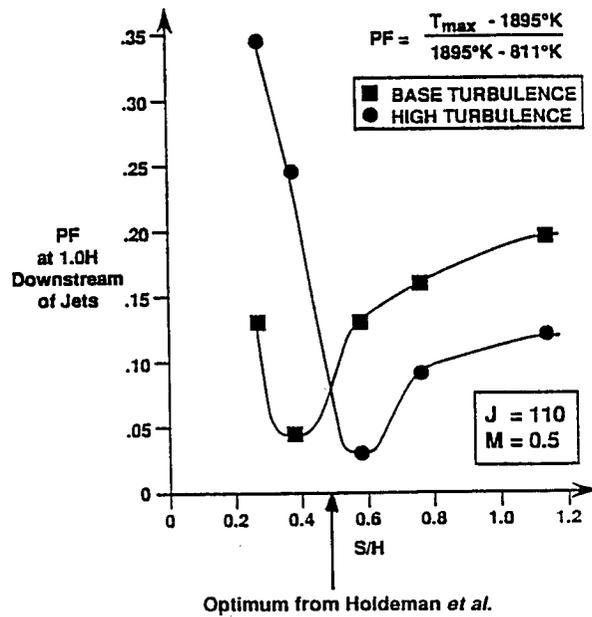
Figure 28. Pattern Factor Results from CFD Analysis of
Combustor Dilution Zone [19]

To make an objective comparison, the optimum conventional mixer must be compared to AJP designs. This necessitated finding the optimum J for the conventional mixer and then using the same J for AJP analysis. Initial non-reacting studies showed J = 32 to be optimum for the twelve slot geometry and hence it was selected for the AJP studies. Later findings showed that J = 40 was optimum for the reacting flows, but time did not permit using J = 40 for AJP analysis. It is felt that using J = 32 does not invalidate the comparative studies between conventional and AJP concepts.

5.1   Geometry

Two AJP configurations were numerically tested as shown schematically in Figure 4. The first configuration consisted of a single jet injected towards the centerline of the can. The second configuration consisted of three jets injected into the mix section: one central jet and two jets injected parallel but opposite in direction to the central jet. Due to geometric symmetry, the calculation domain was reduced to half the circular duct with a central angle of 180 degrees. The transverse boundaries were set to slip walls. The spacing-to-diameter ratio of the jets was arbitrarily selected to be 0.707, based on engineering intuition.

38

5.2   Grid

The grid was composed of 55,296 cells (32×16×108), and chosen to be consistent with the conventional mixer grids in terms of grid density. A typical cross sectional view of an AJP rθ grid is shown in the Figure 29. Figure 29 also shows the location of the two jets with respect to the domain. Note that the plane of symmetry divides the central jet into two halves. The axial grid distribution is similar to that of the conventional mixer.

Jet ⟶

Jet ⟵
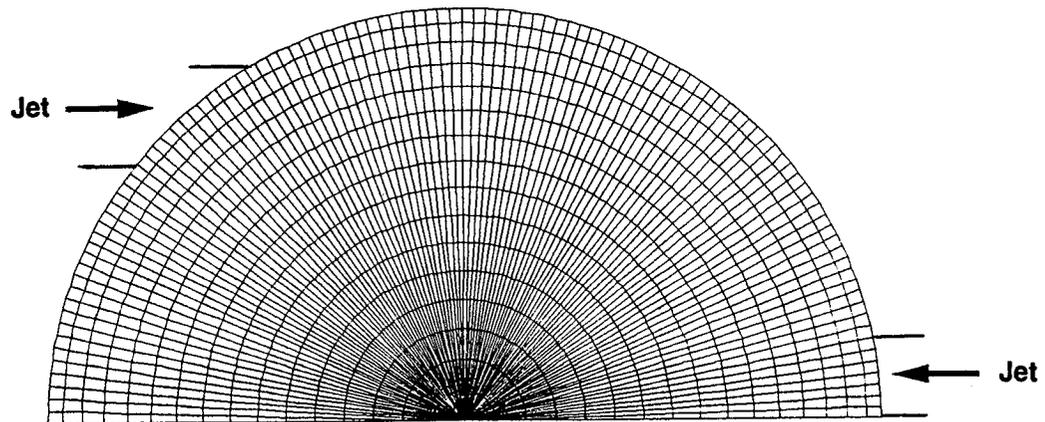
Figure 29.   rθ Grid Used for AJP Calculations

5.3   Numerical Details

The same numerics and models were employed as discussed previously in the conventional mixer analysis. The inlet conditions including the turbulence parameters were the same as the conventional mixer case. Since the REFLEQS code solves for the contravariant components, the cartesian velocity components were transformed into corresponding components based on the local grid curvature.

Since the number of slots was reduced to one or three in the AJP configurations (as compared to twelve slots of the conventional mixer), the slot area was increased to maintain the same total mass flow through the slots. For the case of the three-jet configuration, the slots were not assumed to be the same size. Since the central jet is located at the maximum height location, it needs to travel a greater distance before it

can impinge on the opposite wall. Taking this fact into consideration, the mass flow was split between the central jet and the other two jets in the ratio 2:1:1.

Full convergence of all residuals was attained for each case. Convergence took nearly 40 CPU hours on the Alliant FX/8. Convergence characteristics observed were very similar to that of the conventional mixer.

5.4 Results

Results for both the one-jet and three-jet AJP schemes are discussed below. Isothermal color maps of each case analyzed are presented in Appendix A.

One-Jet Configuration. The one-jet configuration produced a jet that penetrated through the center line, impinging on the opposite side, and split in half. One large vortex cell was produced on the semi-circular cross-section. Mixing scales were much larger for this case compared to the conventional mixer. Figure 30 shows isotherms in several axial planes downstream of the jet: x/D = 0.0, 0.5, 1.0, and 2.0. One characteristic feature of the dilution jet which can be observed is the formation of the familiar kidney shaped structure as the flow proceeded downstream.

Three-Jet Configuration. The mixing in the one-jet configuration can be enhanced by splitting up the single jet into three jets and creating multiple vortex cells. Both reacting and non-reacting flow cases were tested for the three-jet AJP configuration at J = 32. For the non-reacting case, isotherms are presented at x/D = 0.0, 0.5, and 1.0 in Figure 31. It can be noted that there was a single zone of high temperature in the domain. This location corresponded to the region blocked by the central jet as it entered the mainstream.

For the reacting case, isotherms are shown in Figure 32. As in the non-reacting case, all the high temperature isotherms were located downstream of the jet entrance. It appears that the jet behaved like a flameholder, and extended reaction took place in the recirculation zone in the wake of the jet. In locations other than this particular zone, the temperatures were relatively low and uniform, indicating very good mixing. The MWSD for this configuration was 0.033 at x/D = 2.0. However, due to the hot streak, the EI was 4.24.
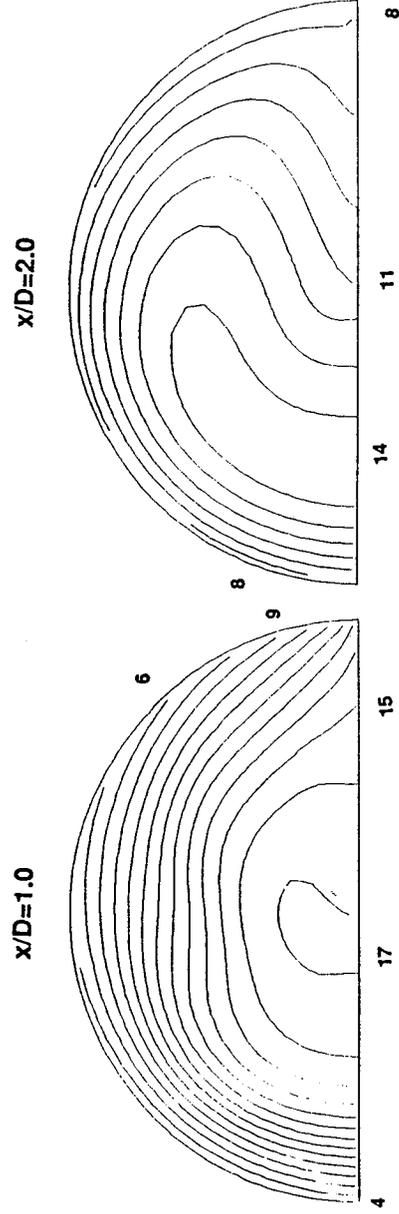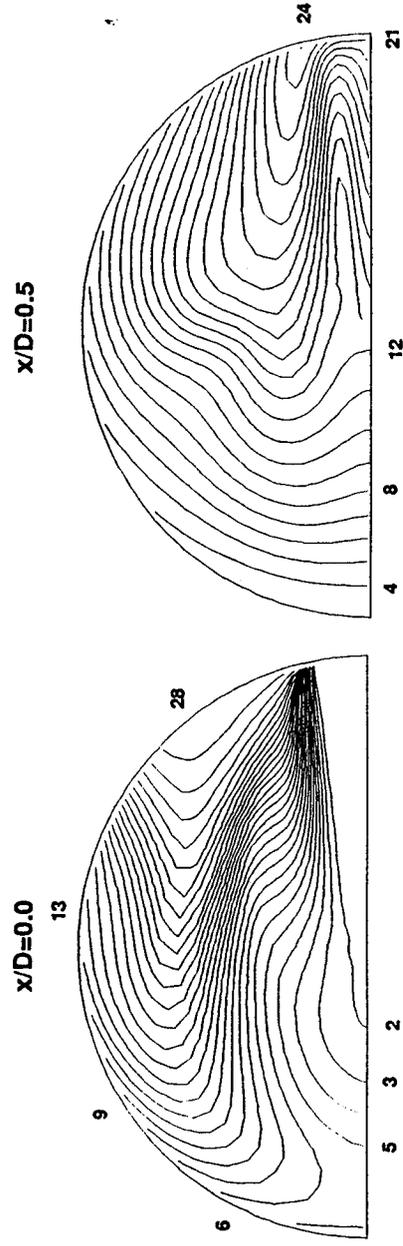
x/D=0.5

x/D=0.0

x/D=2.0

x/D=1.0

CONTOUR LEVELS

1	800
3	900
5	1000
7	1100
9	1200
11	1300
13	1400
15	1500
17	1600
19	1700
21	1800
23	1900
25	2000
27	2100
29	2200
31	2300

Figure 30. Isotherms Predicted for One-Jet AJP
Configuration: Non-Reacting Flow

41

x/D=0.0

x/D=0.5

x/D=1.0

x/D=2.0

CONTOUR LEVELS

1	800
3	900
5	1000
7	1100
9	1200
11	1300
13	1400
15	1500
17	1600
19	1700
21	1800
23	1900
25	2000
27	2100
29	2200
31	2300
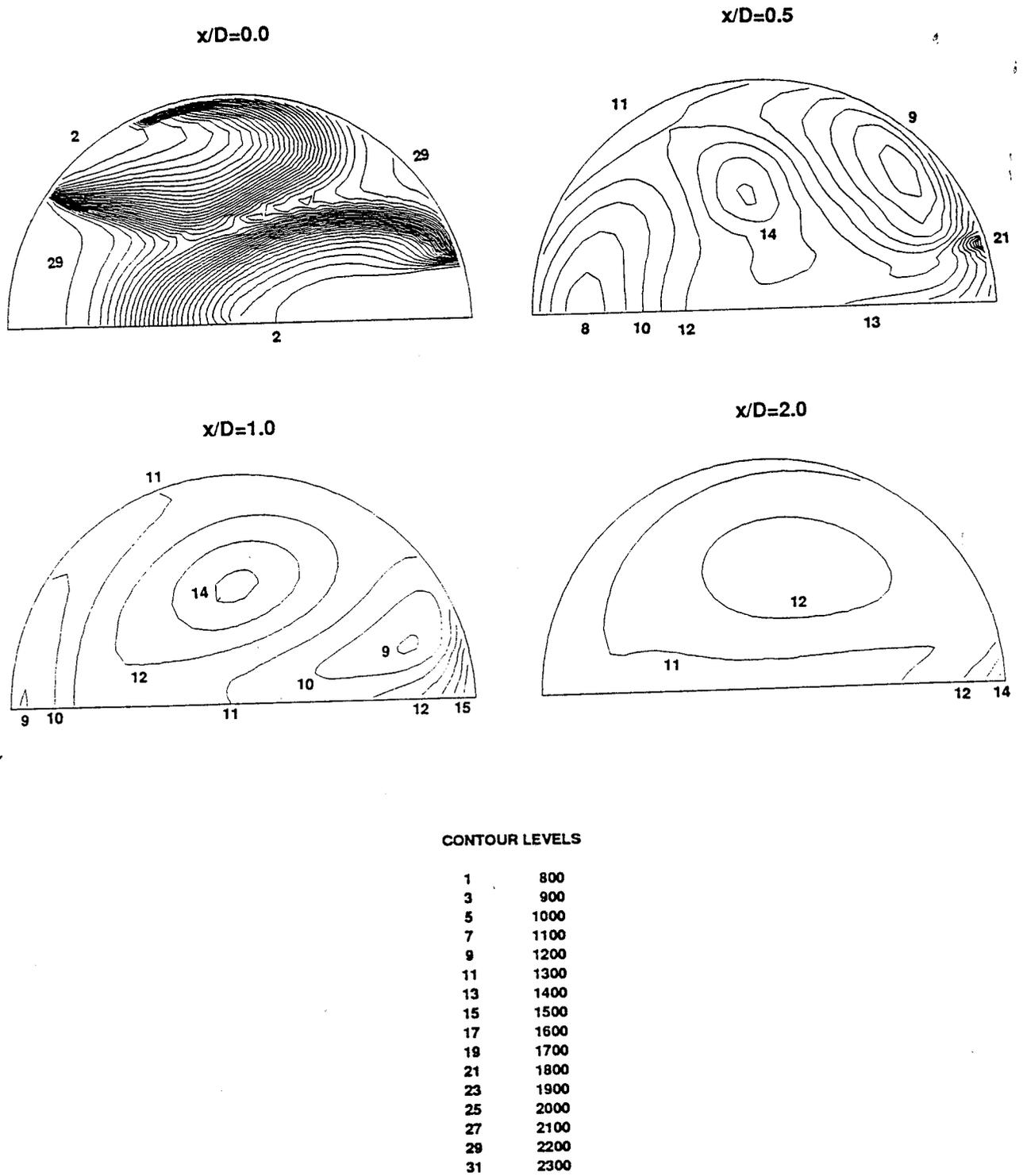
Figure 31. Isotherms Predicted for Three-Jet AJP
Configuration: Non-Reacting Flow
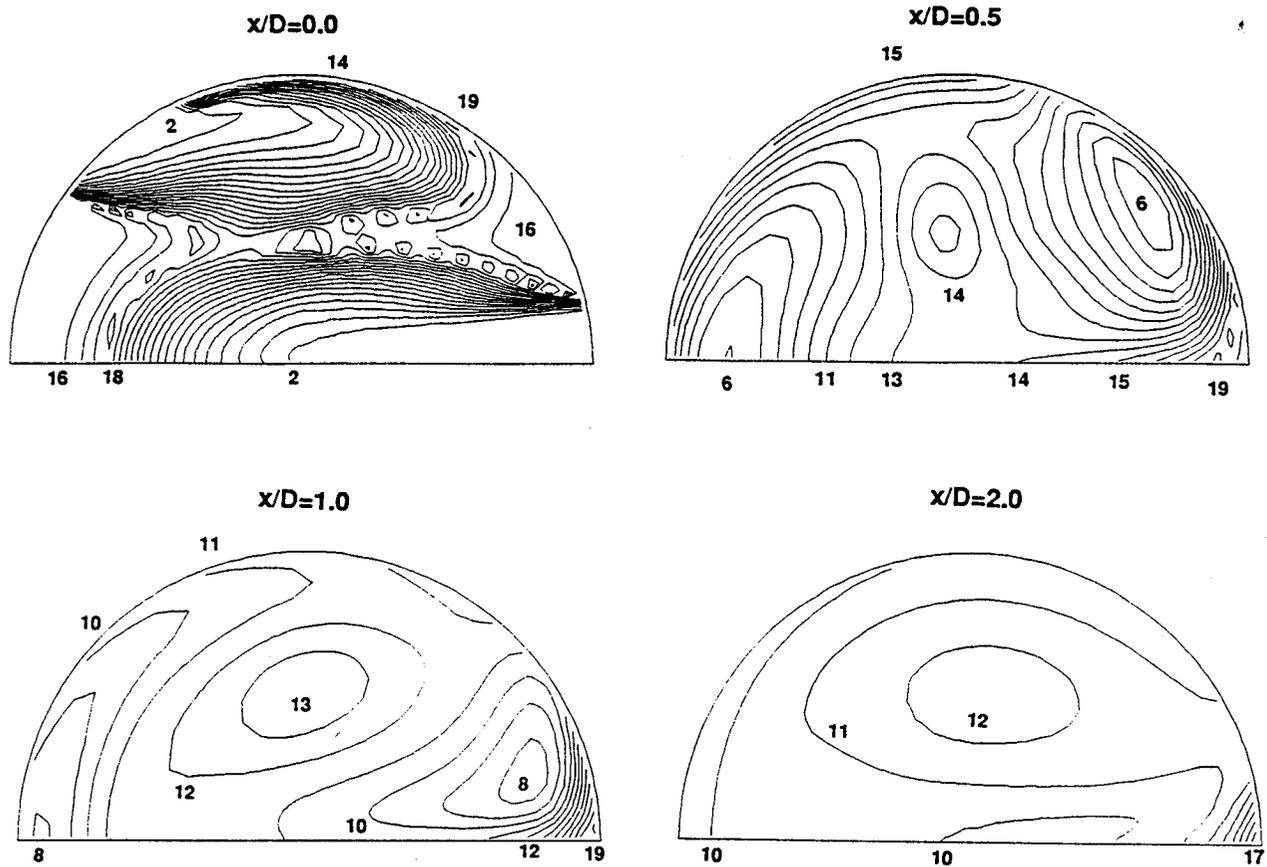
42

x/D=0.0

x/D=0.5

x/D=1.0

x/D=2.0

CONTOUR LEVELS	
1	800
2	900
3	1000
4	1100
5	1200
6	1300
7	1400
8	1500
9	1600
10	1700
11	1800
12	1900
13	2000
14	2100
15	2200
16	2300
17	2400
18	2500
19	2600
20	2700

Figure 32.   Isotherms Predicted for Three-Jet AJP
Configuration: Reacting Flow

43

6. COMPARISON AND EVALUATION OF AJP CONCEPT

CFD analysis of the conventional mixer and the three-jet AJP configuration for the J = 32 case have been performed. For non-reacting flows, Figure 33 compares isotherms of the two designs at x/D = 1.0 and 2.0. The important observation one can make is the location of high temperature zones. For the conventional mixer, the high temperature zone is located in the center of the duct, but for the AJP design it is located in one small region on the combustor wall. For quantitative comparison, the MWSD of temperature for the two cases is shown in Table 1. The AJP is clearly shown to be superior in terms of overall mixing.

For reacting flows, Figure 34 compares isotherms between conventional and AJP designs at x/D = 1.0 and 2.0. The range of temperatures for the AJP concept is greater than that of the conventional mixer, but most of the high temperatures are located in a narrow zone located in the wake of the central jet. AJP appears to be a better mixer except for this single streak of high temperatures. The comparison of the MWSD for the two cases is shown in the Table 2. Again, AJP is much better than the conventional configuration in terms of overall mixing.

However, the AJP concept is inferior in terms of NO_x generation. The high local temperature zone helps generate high levels of NO_x and deteriorates the emission performance of the mixer. The calculated NO_x concentrations and emission index levels are shown in Table 3.

The inference one can make is good mixing (in terms of MWSD) is not necessarily the only criteria for low NO_x formation. Stray hot spots can generate large amounts of NO_x and must be avoided. It is possible that non-reacting experiments often performed to screen designs may produce misleading results if only MWSD is used as the "goodness" criteria. Perhaps a better mixing criteria should be both MWSD and PF (for definition see page 3-4). Table 4 compares PF between concepts for non-reacting flow. The AJP concept is inferior to the conventional design. For one quick-mix design to be better than another, it should have both lower MWSD and PF.

Because of its enhanced overall mixing capabilities, it seems logical not to drop the AJP concept from consideration. Instead, it might be possible to make minor adjustments to

CONVENTIONAL

x/D=1.0
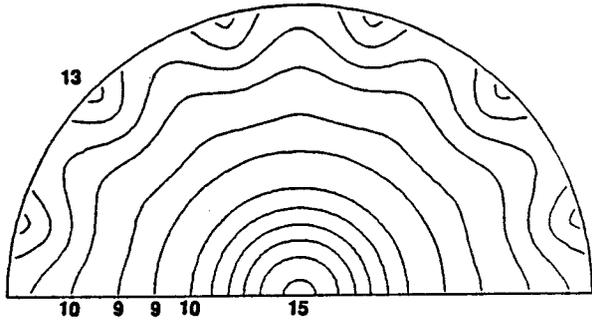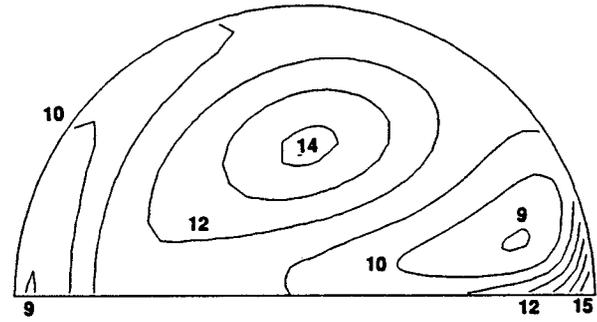
AJP

x/D=1.0

CONTOUR LEVELS

1	800
3	900
5	1000
7	1100
9	1200
11	1300
13	1400
15	1500
17	1600
19	1700
21	1800
23	1900
25	2000
27	2100
29	2200
31	2300

x/D=2.0
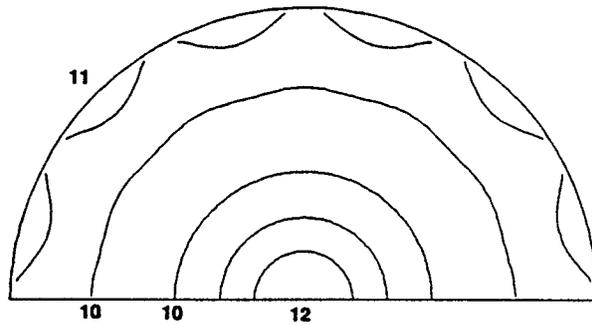
x/D=2.0
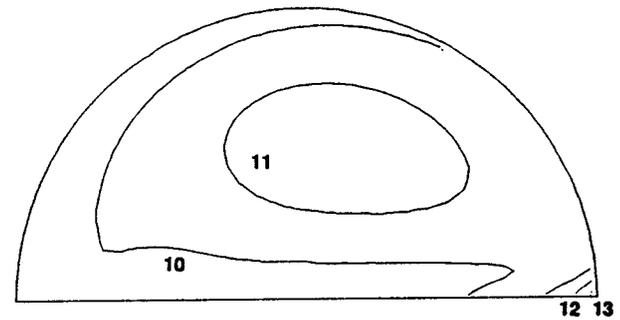
Figure 33. Comparison of Three-Jet AJP and Conventional
Designs: Non-Reacting Flow

CONVENTIONAL

x/D=1.0
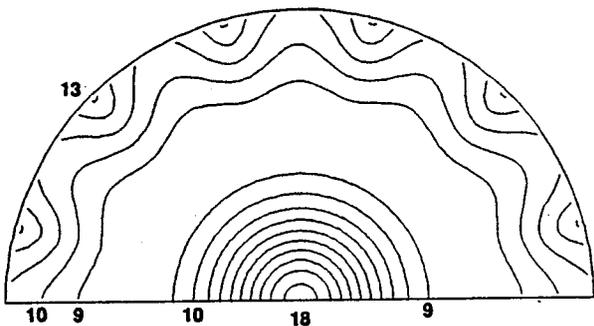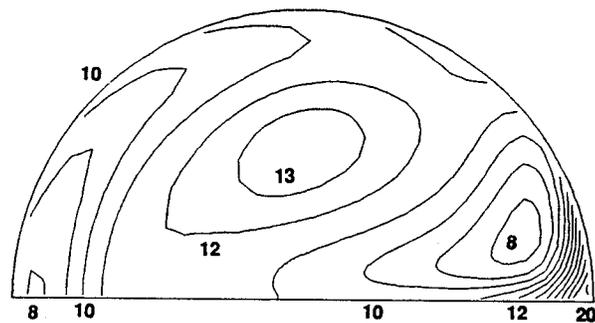
AJP

x/D=1.0

CONTOUR LEVELS	
1	800
2	900
3	1000
4	1100
5	1200
6	1300
7	1400
8	1500
9	1600
10	1700
11	1800
12	1900
13	2000
14	2100
15	2200
16	2300
17	2400
18	2500
19	2600
20	2700

x/D=2.0
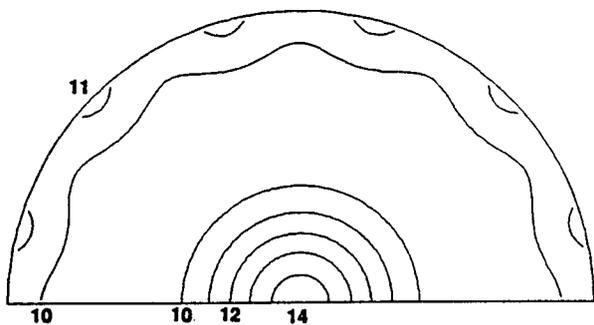
x/D=2.0
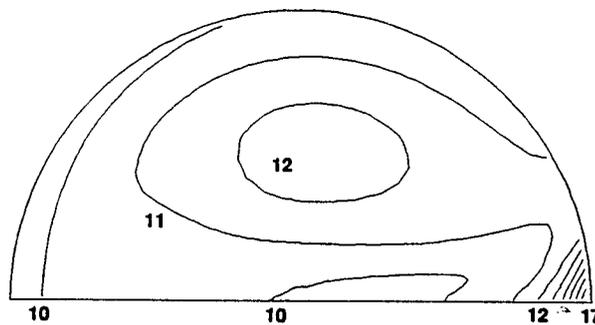
Figure 34. Comparison of Three-Jet AJP and Conventional

Table 1.   Predicted MWDF of Temperature: Non-Reacting Flow

	x/D = 1.0	x/D = 2.0
AJP CONCEPT	0.032	0.015
CONVENTIONAL MIXER	0.089	0.043

Table 2.   Predicted MWSD of Temperature: Reacting Flow

	x/D = 1.0	x/D = 2.0
AJP CONCEPT	0.062	0.033
CONVENTIONAL MIXER	0.183	0.102

Table 3.   Predicted Emission Levels

	x/D = 1.0		x/D = 2.0	
	EI	NOx (ppm)	EI	NOx (ppm)
AJP CONCEPT	3.95	541	4.24	579
CONVENTIONAL MIXER	3.03	415	3.31	453

Table 4.   Predicted Pattern Factor: Non-Reacting Flow

	x/D = 1.0		x/D = 2.0	
	PF	MWSD	PF	MWSD
AJP CONCEPT	0.57	0.032	0.37	0.015
CONVENTIONAL MIXER	0.49	0.089	0.24	0.043

4090/1-003CAB

47

the slot design to eliminate the "flameholder" effect, but still maintain good overall mixing. Possible design modifications include slot shape (an aerofoil shape instead of a rectangular slot), slot aspect ratio (a larger aspect ratio would reduce jet blockage), flow split between the slots, and slot spacing.

7. CONCLUSIONS

The overall conclusions of this Phase I study are:

1. The viability of using 3-D CFD to model quick-mix concepts of a low emission combustor was successfully demonstrated.

2. A conventional five-inch diameter quick-mix section compatible with the NASA LeRC Low Emission Combustor Program was numerically analyzed. The conventional configuration consisted of twelve, radial-inflow slots uniformly distributed around the perimeter of the quick-mix section. Optimum mixing for non-reacting flow occurred for a jet-to-mainstream momentum flux ratio (J) of 32. For reacting flow, the NO_2 emission index (EI) was, shown to be highly sensitive to J, with the lowest value of 2.9 calculated for J of 40 (at x/D = 2.0). For J of 32, the EI was 3.3.

3. Two configurations of the Asymmetric Jet Penetration (AJP) concept were numerically analyzed for J of 32. The best configuration consisted of a three-jet arrangement producing large scale counter-rotating vortices. The mixing effectiveness for non-reacting flow (defined as the Mass-Weighted Standard Deviation, MWSD, of temperature), was 0.015 compared to 0.043 for the conventional case at x/D = 2.0. For reacting flow, the AJP concept produced a mixing effectiveness of 0.033 compared to 0.102 for the conventional case. However, the EI was higher for the AJP concept compared to the conventional design, 4.2 to 3.3. This was caused by a singular hot streak downstream of the central jet entry location. Minor slot modifications were identified that have the potential of eliminating the hot streak while still maintaining superior mixing characteristics. Further study is needed to screen the AJP design, including parametric variation of key design features (*e.g.* slot spacing, slot aspect ratio, slot shape *etc.*).

4. The results of this study have shown that there may be errors in evaluating low NO_x mixing concepts under non-reacting flow conditions if the only

48

criteria is MWSD. It is recommended that pattern factor (or some other form of assessing local hot spots) should also be used as a screening criteria.

8. RECOMMENDATIONS FOR PHASE II

The work performed in Phase I has established a good foundation for Phase II study. The viability of using 3-D CFD analysis to evaluate advanced mixing concepts has been demonstrated. The probability of identifying concept(s) with enhanced mixing in RQL combustors is high if Phase II is awarded.

The three-jet AJP mixing concept was shown to have superior mixing characteristics compared to conventional slots, but excessive NO_x was predicted. Higher levels of NO_x were caused by a local "hot" spot in the wake of the central jet. Ways of maintaining good mixing but eliminating the local "hot" spot have been identified for CFD analysis in Phase II. Also in Phase II, another advanced mixing concept will be screened: the lobed mixer. The lobed mixer has demonstrated increased mixing in turbofan afterburner geometries, and has good potential for quick-mix applications.

Both AJP and lobed mixer concepts will be analyzed (using CFD) and evaluated against each other and baseline configurations. Both can and annular geometries will be studied. The "best" configurations will be experimentally tested under non-reacting flow conditions. Planar imaging data will be obtained, from which mixedness and "hot spot" parameters will be calculated. The best concept(s) will be selected for hot testing in the NASA LeRC RQL flametube combustor.

Tasks envisioned for Phase II are:

1. Analysis of mod-AJP concepts;
2. Analysis of lobed mixer concepts;
3. Analysis of slanted-slot (baseline) concept;
4. Analysis of concepts for annular combustors;
5. Evaluation and selection of quick-mix concepts for experimental tests;
6. Experimental tests under non-reacting flow conditions;
7. Optimization analyses; and

8. Preliminary design of concept(s) for NASA LeRC RQL flametube combustor.

9. REFERENCES

1. R. E. Jones, "Gas Turbine Engine Emissions - Problems, Progress and Future," *Prog. Energy Combust. Sci.* 4, pp. 73-113, 1978.

2. R. R. Tacina, "Low NO_x Potential Of Gas Turbine Engines," AIAA-90-0550, 28th Aerospace Sciences Meeting, January 8-11, 1990.

3. H. Nguyen, D. Bittker, and R. Niedzwiecki, "Investigation of Low NO_x Staged Combustor Concept in High Speed Civil Transport Engines," AIAA-89-2942, AIAA/ASME/SAE/ASEE 25th Joint Propulsion Conference, July 10-12, 1989.

4. J. D. Holdeman, "A Numerical Study of the Effects of Curvature and Convergence on Dilution Jet Mixing," AIAA-87-1953, AIAA/SAE/ASME/ASEE 23rd Joint Propulsion Conference, June 29 - July 2, 1987.

5. A. J. Przekwas, and S. D. Habchi, "Computer Model of a Jet Embedding and Eulerian-Lagrangian Techniques for Simulating Reactive Fluid Dynamics in Liquid Rocket Engines," NASA SBIR Contract NAS8-37321, July 1987.

6. A. J. Przekwas, *et al.*, "Improvements to a Computer Program for Simulation of Liquid Rocket Engines," NASA SBIR Contract NAS3-25123, September 1987.

7. B. E. Launder, and D. B. Spalding, "The Numerical Computation of Turbulent Flows," *Computer Methods in Applied Mechanics and Engineering*, Vol. 3, pp. 269-289, 1974.

8. Y. -S. Chen, and S. -W. Kim, "Computation of Turbulent Flows Using an Extended k-ϵ Turbulence Closure Model, NASA CR-179204, October 1987.

9. S. -W. Kim, and C. P. Chen, "A Multiple Time Scale Turbulence Model Based on Variable Partitioning of Turbulent Kinetic Energy Spectrum," AIAA-88-1771, 1988.

10. K. Y. Chien, "Predictions of Channel and Boundary-Layer Flows with a Low-Reynolds-Turbulence Model," *AIAA Journal*, Vol. 23, No. 2, 1985.

11. C. E. Smith, *et al.*, "Validation of an Advanced Turbulent Combustion Code: REFLEQS," 7th SSME CFD Workshop, NASA MSFC, April 1989.

12. M. L. Ratcliff, and C. E. Smith, "REFLEQS-2D: A Computer Program for Turbulent Flow with and without Chemical Reaction; Volume 2: Validation Manual," CFDRC Report GR-88-4, 1989.

13. R. K. Avva, C. E. Smith, and A. K. Singhal, "Comparative Study of High and Low Reynolds Number Versions of k-ϵ Models," AIAA-90-0246, 28th Aerospace Sciences Meeting, Jan 8-11, 1990.

14. R. Srinivasan, "Dilution Jet Mixing Program - Phase II Report," NASA CR-174624, 1984.

15. V. Quan, F. E. Marble, and J. R. Kliegel, "Nitric Oxide Formation in Turbulent Diffusion Flames," 14th Symposium on Combustion, pp. 851-860, 1972.

16. D. Anderson, "Effect of Equivalence Ratios and Dwell Time on Exhaust Emissions from an Experimental Premixed Prevaporizing Burner," NASA TMX-71592, March 1975.

17. G. R. Nickerson, et al., "Two-Dimensional Kinetics (TDK) Nozzle Performance Computer Program; Vol II: Programming Manual," NAS8-36863, March 1989.

18. Experimental Test Plan for the High Speed Research Low NO_x Rich Burn/Quick Quench/Lean Burn Flame Tube Rig in CE-5, ERB, NASA LeRC, March 8, 1990.

19. C. Smith, "Mixing Characteristics of Dilution Jets in Small Gas Turbine Engines," AIAA-90-2728, AIAA/SAE/ASME/ASEE 26th Joint Propulsion Conference, July 16-18, 1990.

20. R. W. Claus, and S. P. Vanka, "Multigrid Calculations of a Jet in Crossflow," AIAA-90-0444, 28th Aerospace Sciences Meeting, Jan. 8-11, 1990.
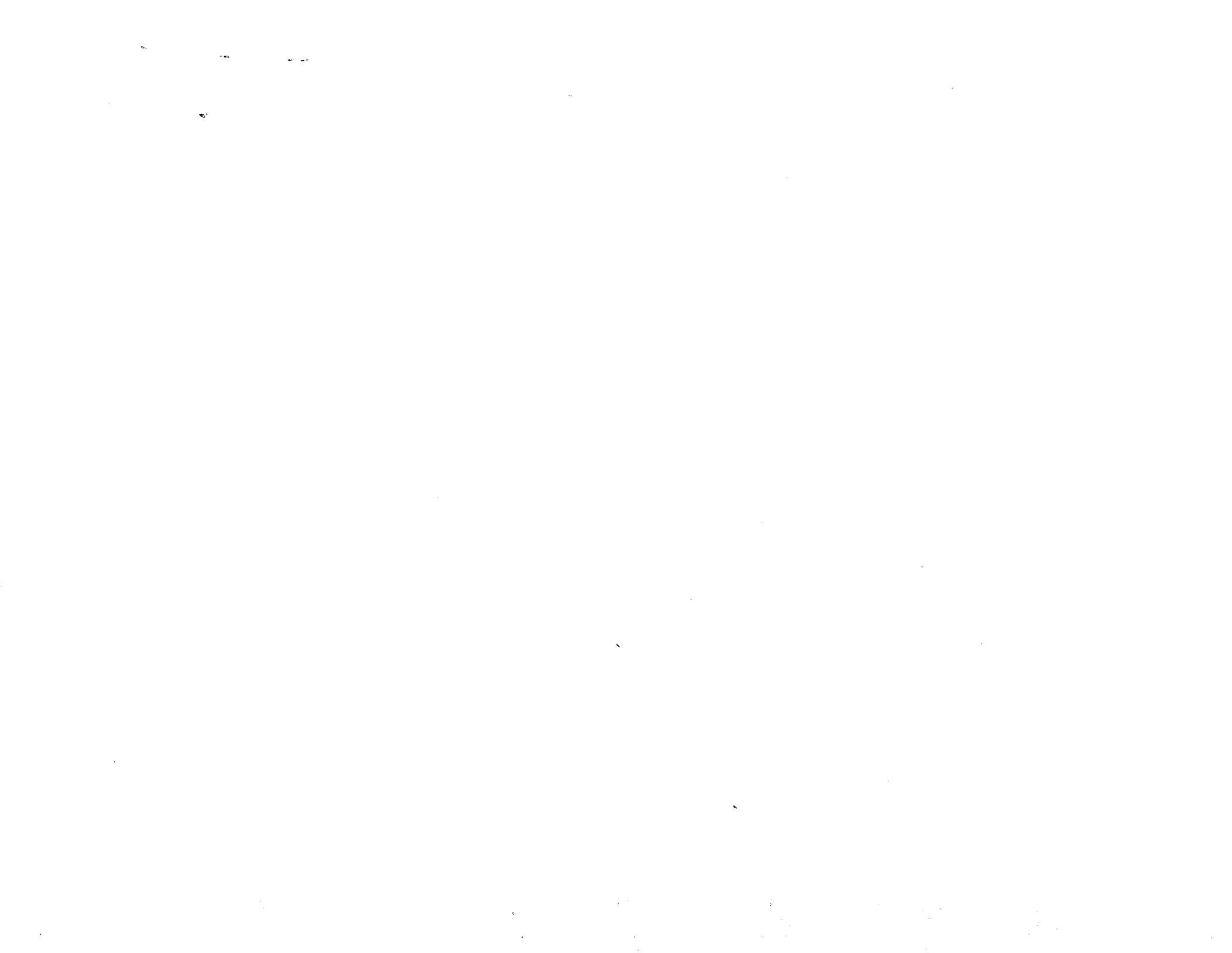
APPENDIX A

Isothermal Color Maps For Each Case Analyzed
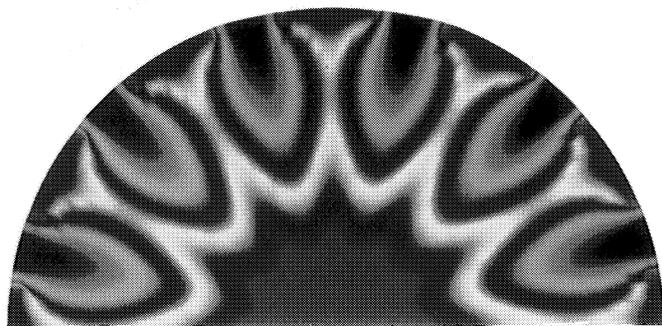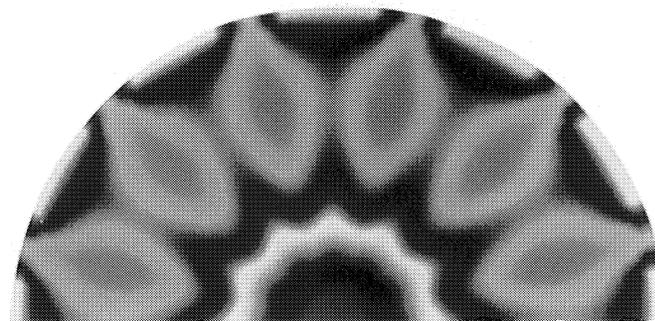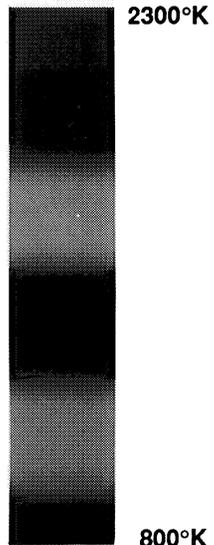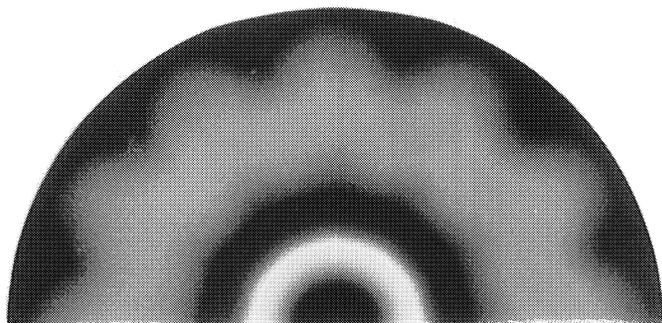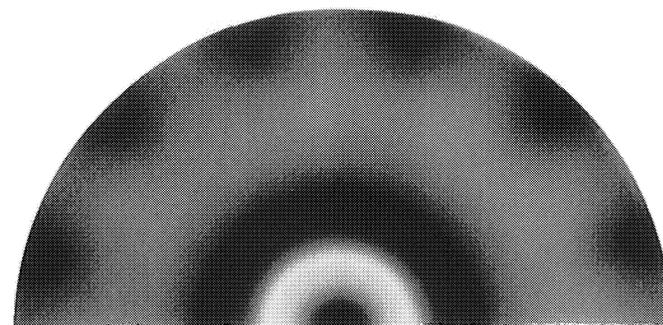
TEMPERATURE CONTOURS

2300°K

800°K

x/D = 0.0

x/D = 0.3

x/D = 1.0

x/D = 2.0

Figure A-1. Non-Reacting Flow: J = 16 (Conventional Mixer Design)

x/D = 2.0

x/D = 1.0

TEMPERATURE CONTOURS

800°K
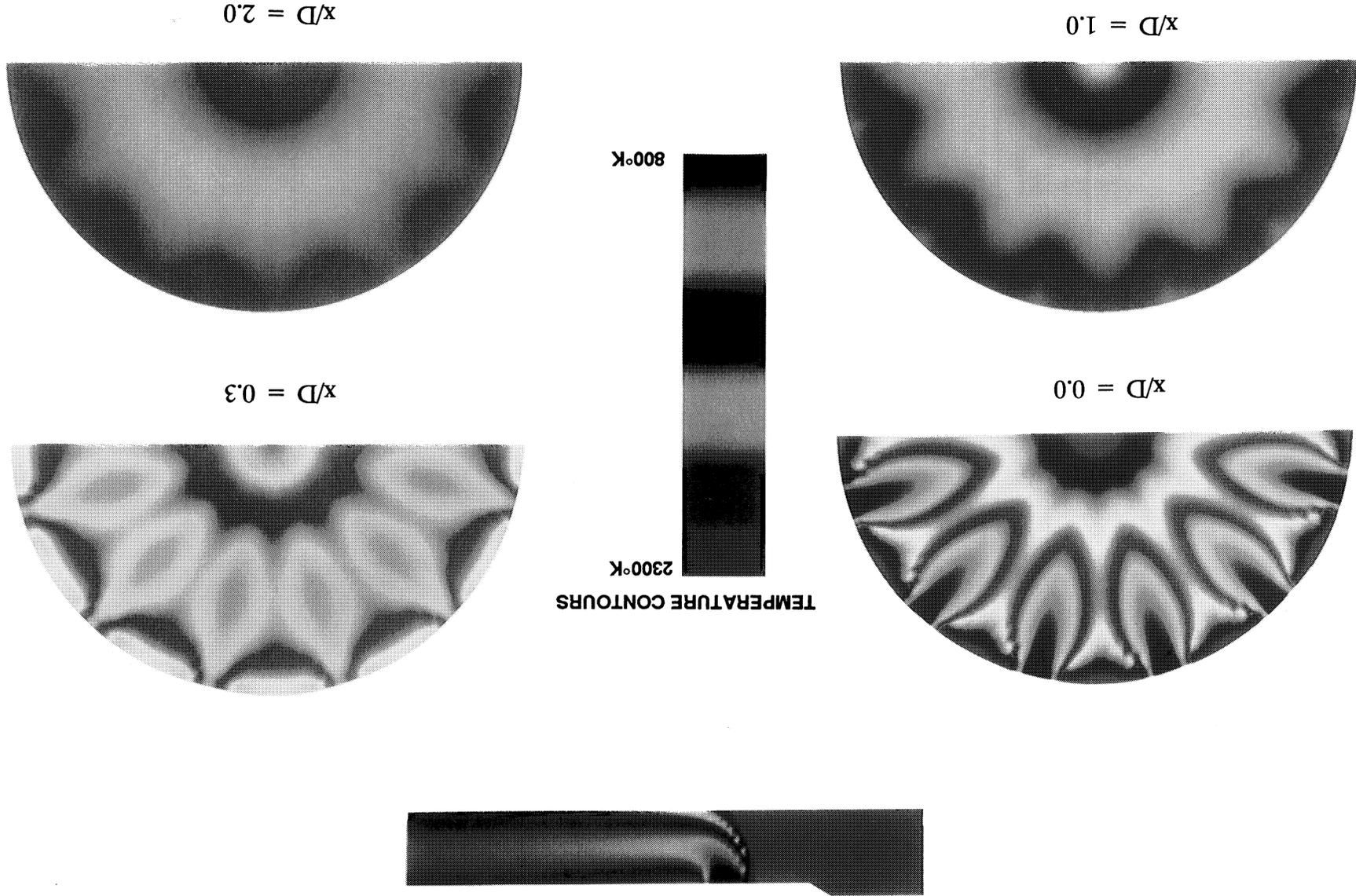
2300°K

x/D = 0.3

x/D = 0.0

Figure A-2. Non-Reacting Flow: J = 32 (Conventional Mixer Design)

56
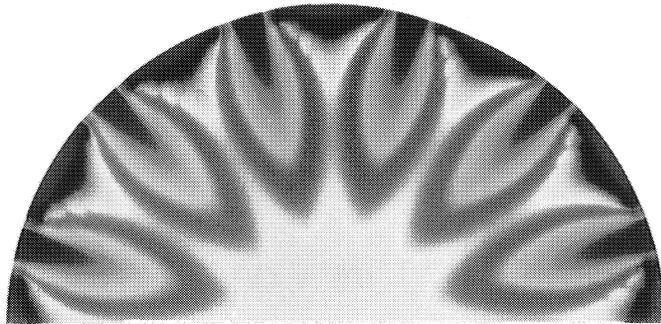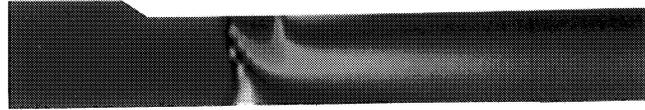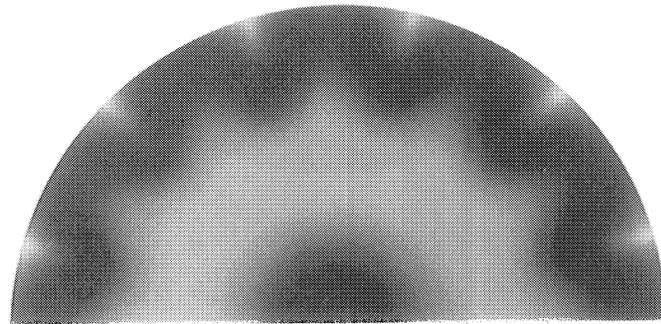
TEMPERATURE CONTOURS
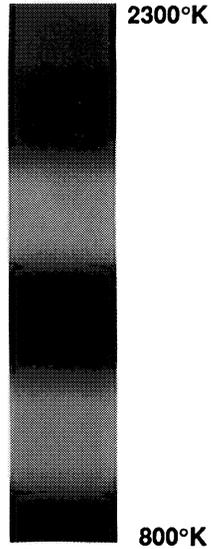
2300°K
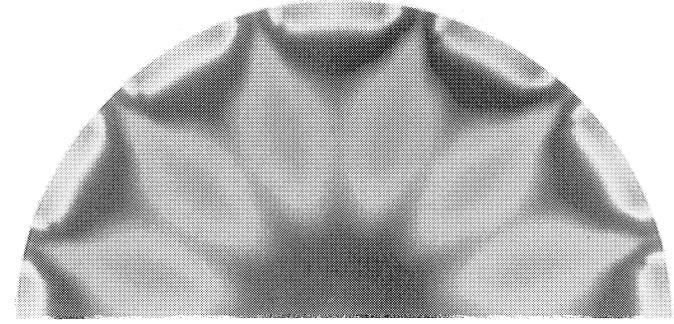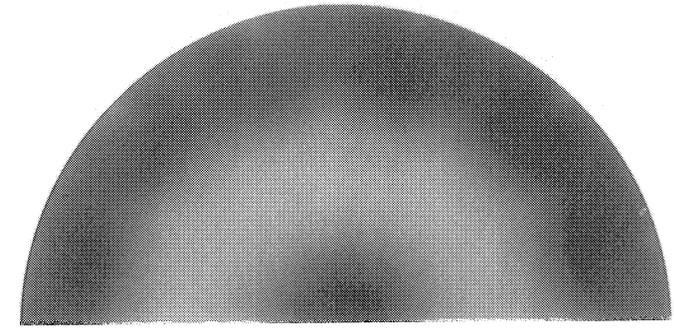
800°K

x/D = 0.0

x/D = 0.3

x/D = 1.0

x/D = 2.0

Figure A-3. Non-Reacting Flow: J = 40 (Conventional Mixer Design)

TEMPERATURE CONTOURS

2300°K

800°K

x/D = 0.0

x/D = 0.3

x/D = 1.0

x/D = 2.0

58
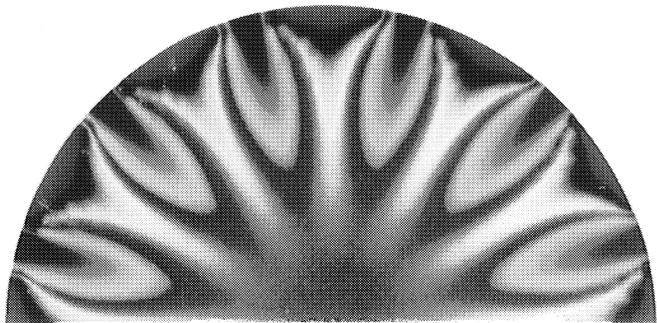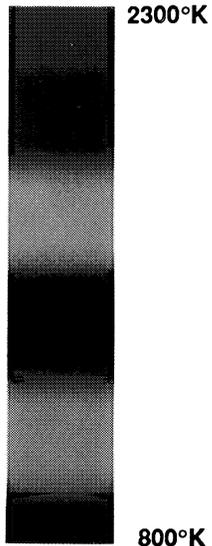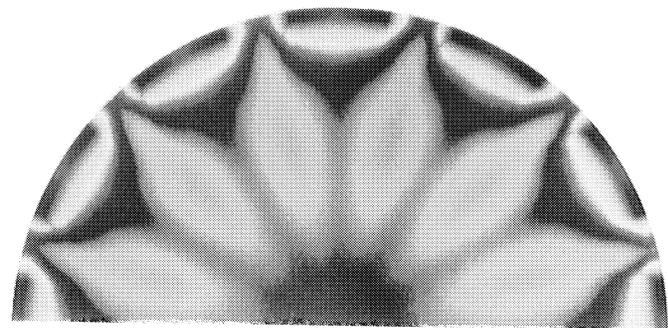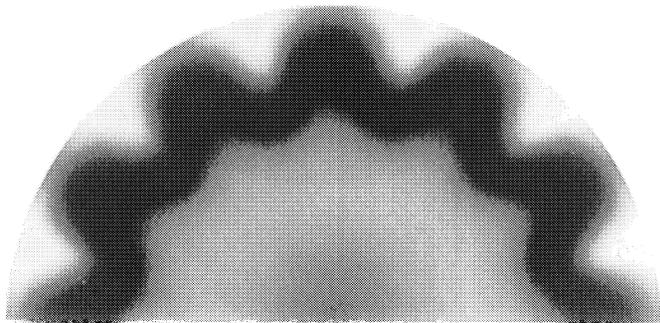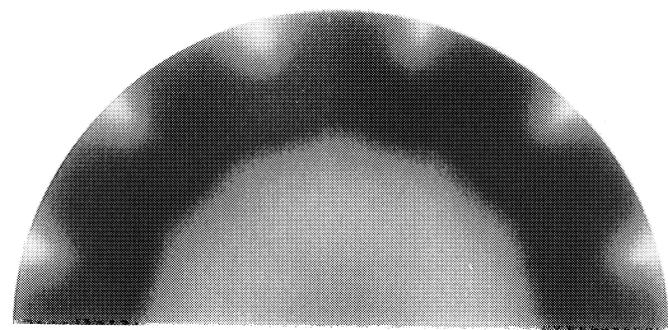
Figure A-4. Non-Reacting Flow: J = 48 (Conventional Mixer Design)

x/D = 2.0

x/D = 1.0

x/D = 0.3

x/D = 0.0

800°K

2300°K

TEMPERATURE CONTOURS
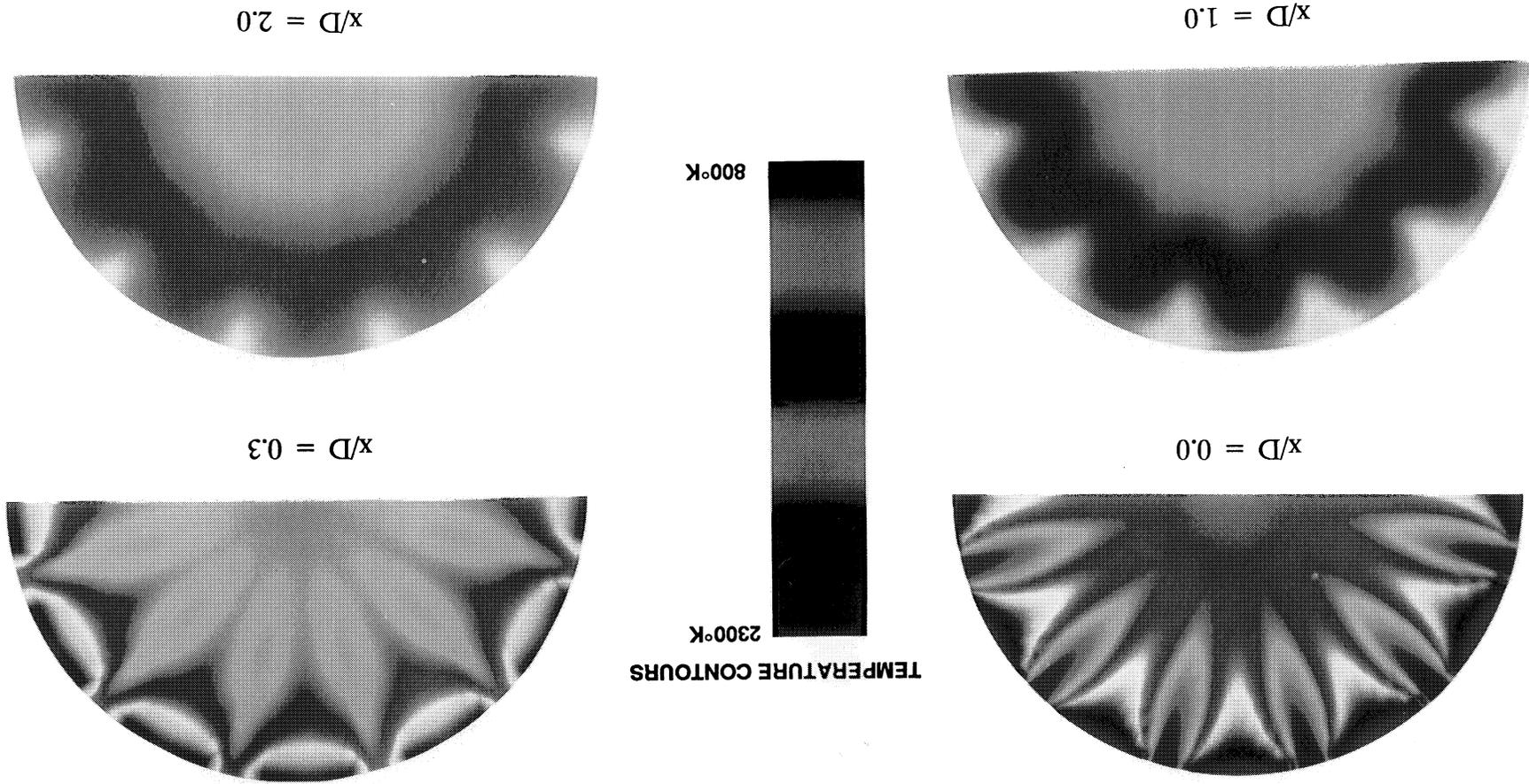
Figure A-5. Non-Reacting Flow: J = 64 (Conventional Mixer Design)

59

TEMPERATURE CONTOURS

2300°K

800°K
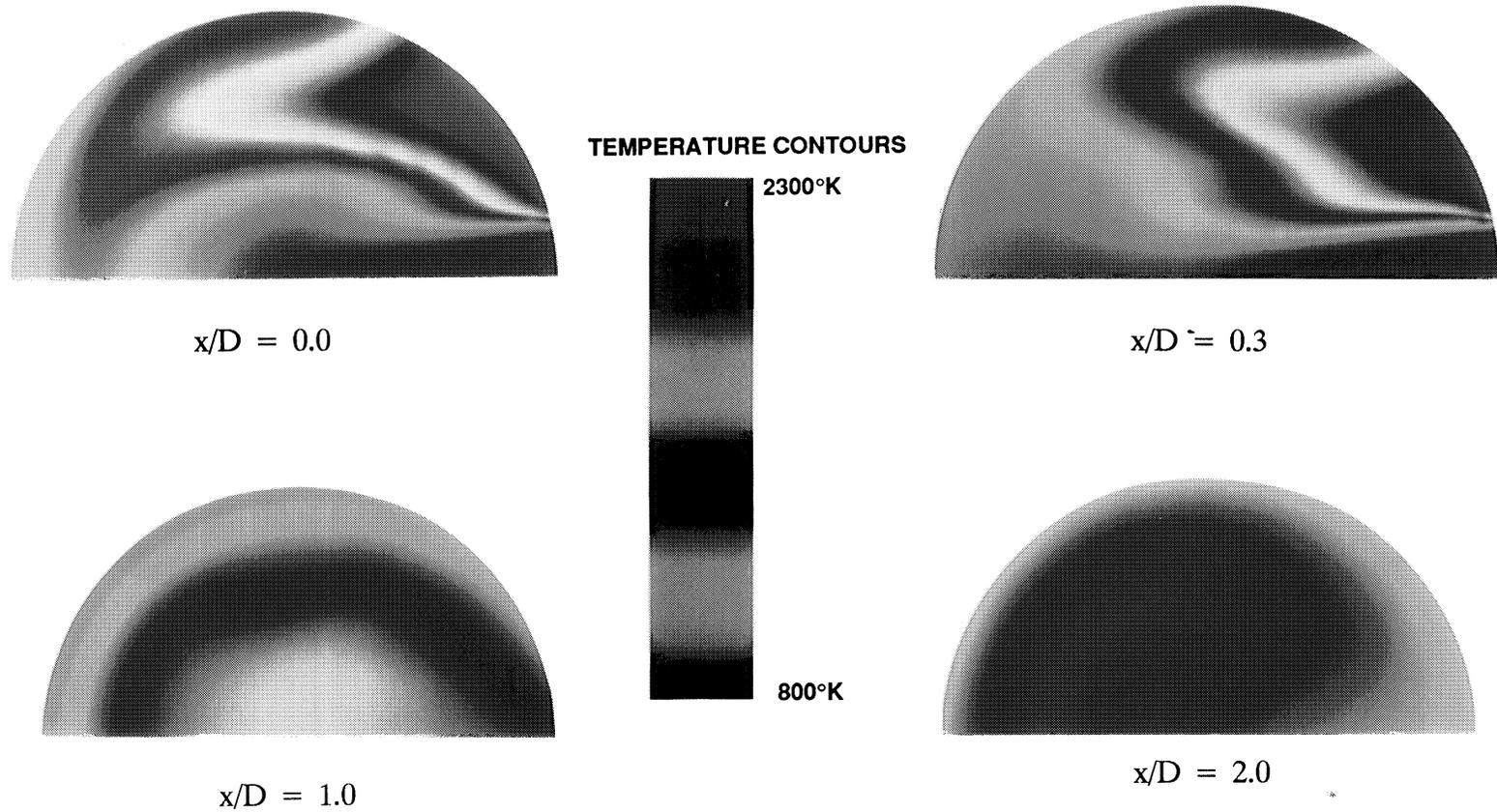
x/D = 0.0

x/D = 0.3

x/D = 1.0

x/D = 2.0

Figure A-6. Non-Reacting Flow: J = 32 (AJP Mixer Design, One-Jet Case)

TEMPERATURE CONTOURS

2300°K

800°K

x/D = 0.0

x/D = 0.3

x/D = 1.0

x/D = 2.0

61
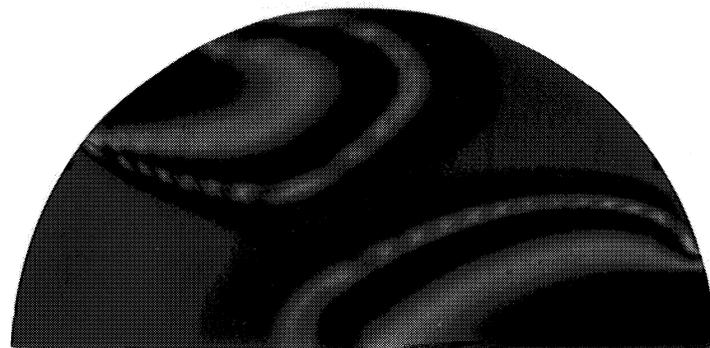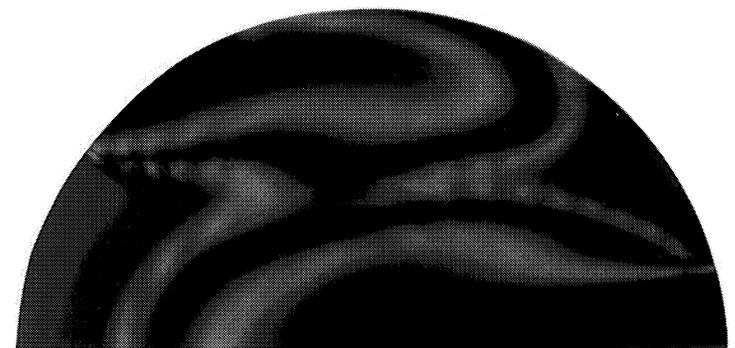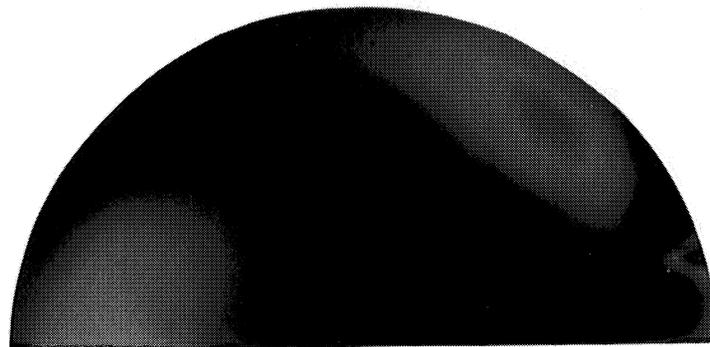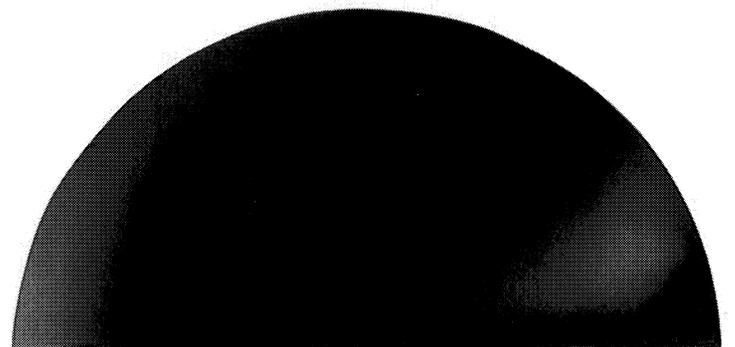
Figure A-7. Non-Reacting Flow: J = 32 (AJP Mixer Design, Three-Jet Case)
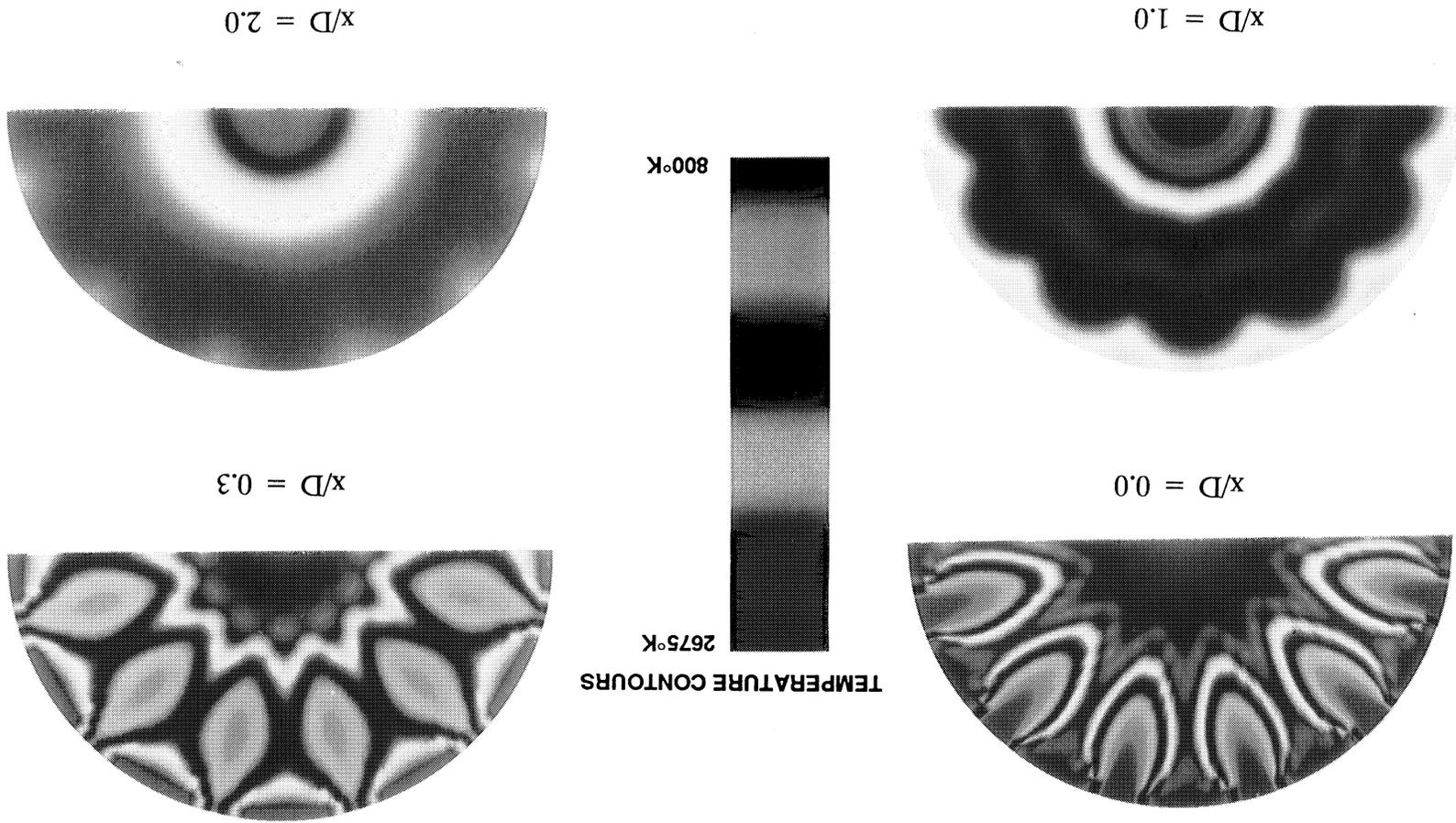
x/D = 2.0

x/D = 1.0

800°K

x/D = 0.3

x/D = 0.0

TEMPERATURE CONTOURS

2675°K

62

TEMPERATURE CONTOURS

2675°K

800°K

x/D = 0.0

x/D = 0.3

x/D = 1.0

x/D = 2.0
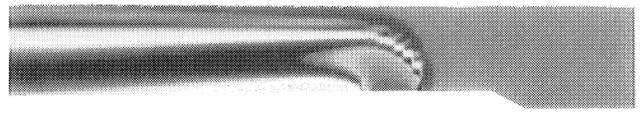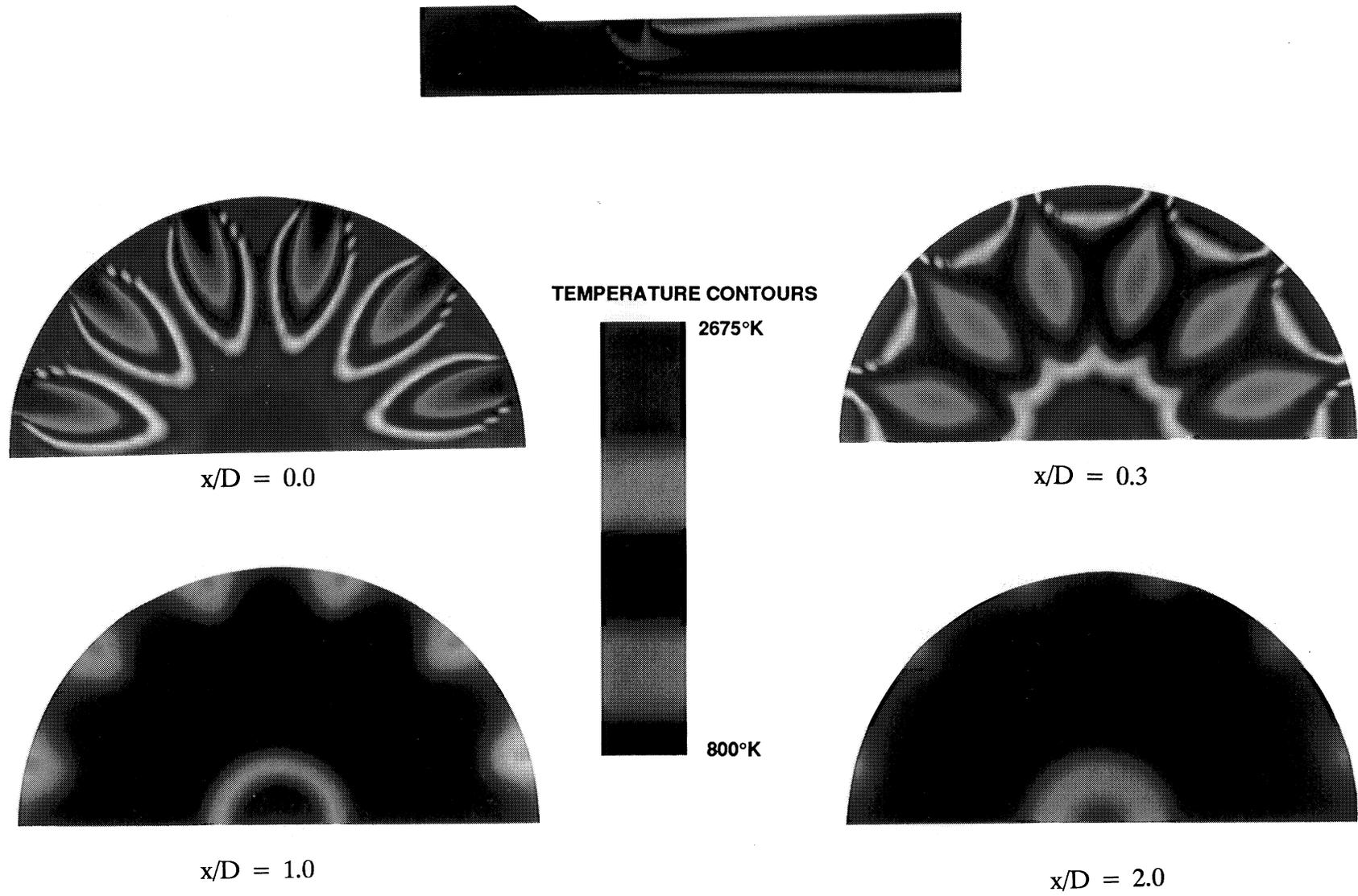
Figure A-9.   Reacting Flow: J = 32 (Conventional Mixer Design)

TEMPERATURE CONTOURS

2675°K

800°K

x/D = 0.0

x/D = 0.3

x/D = 1.0

x/D = 2.0
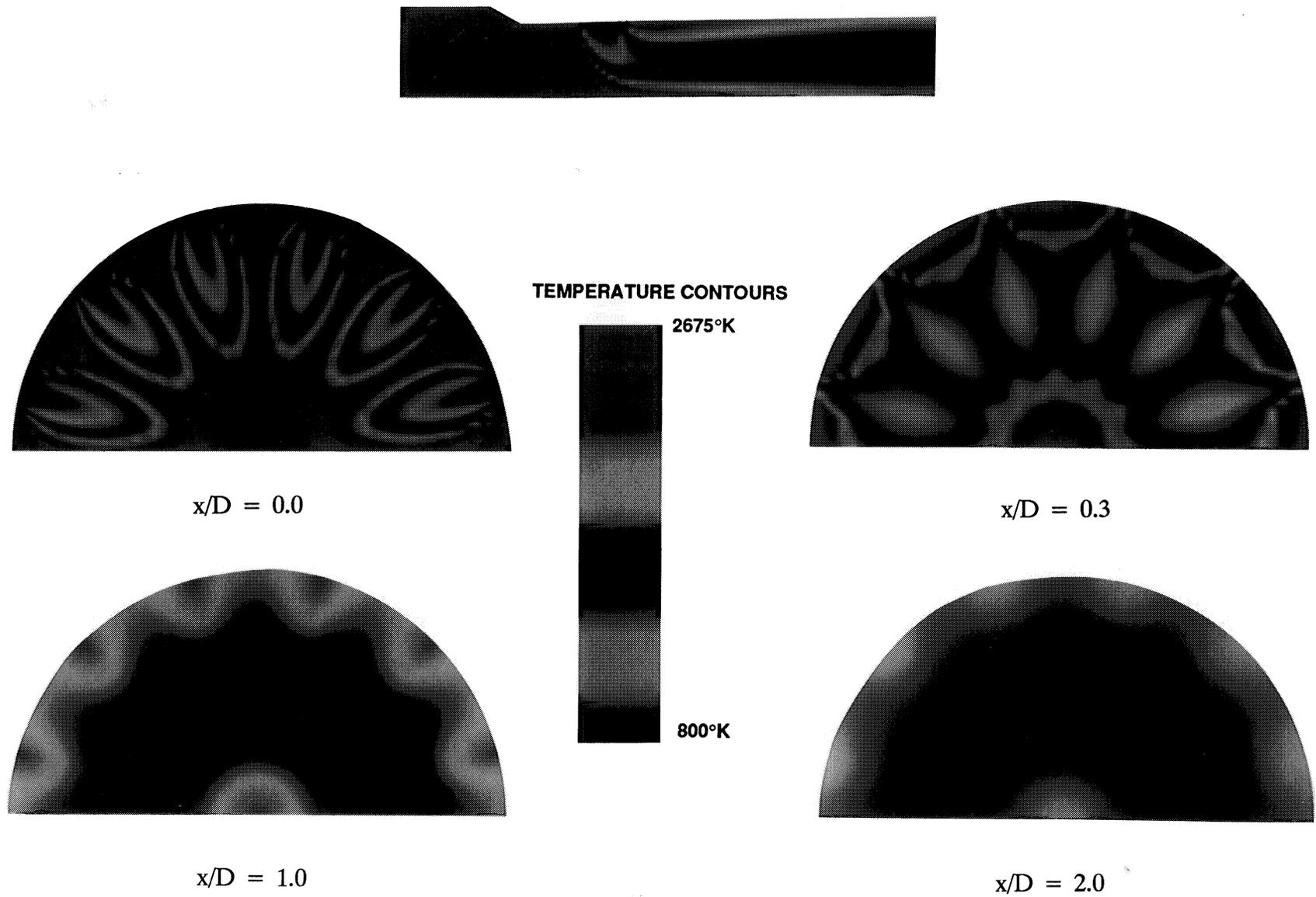
Figure A-10. Reacting Flow: J = 40 (Conventional Mixer Design)

TEMPERATURE CONTOURS

2675°K

800°K

x/D = 0.0

x/D = 0.3

x/D = 1.0

x/D = 2.0
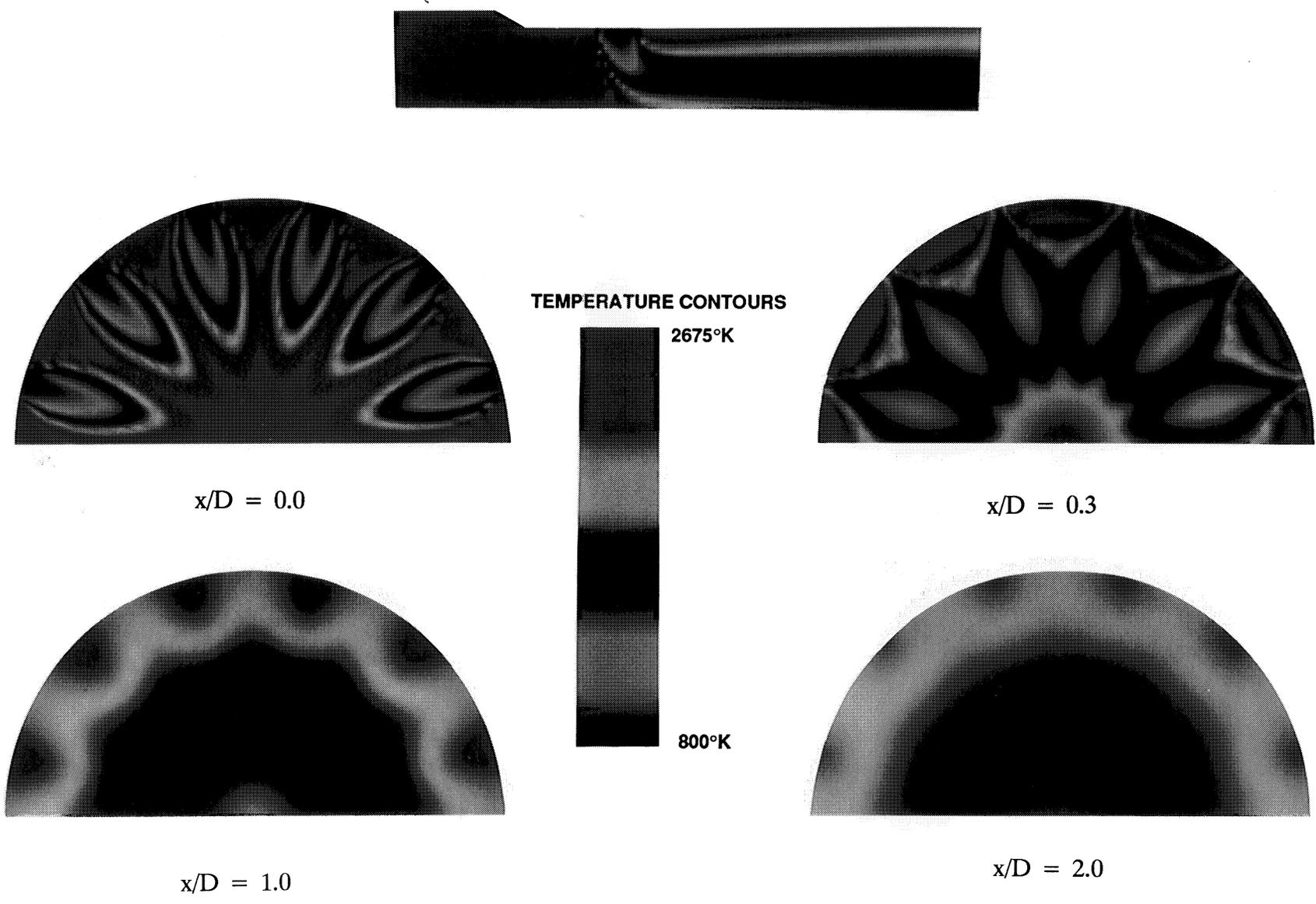
Figure A-11. Reacting Flow: J = 48 (Conventional Mixer Design)

TEMPERATURE CONTOURS

2675°K

800°K

x/D = 0.0

x/D = 0.3

x/D = 1.0

x/D = 2.0
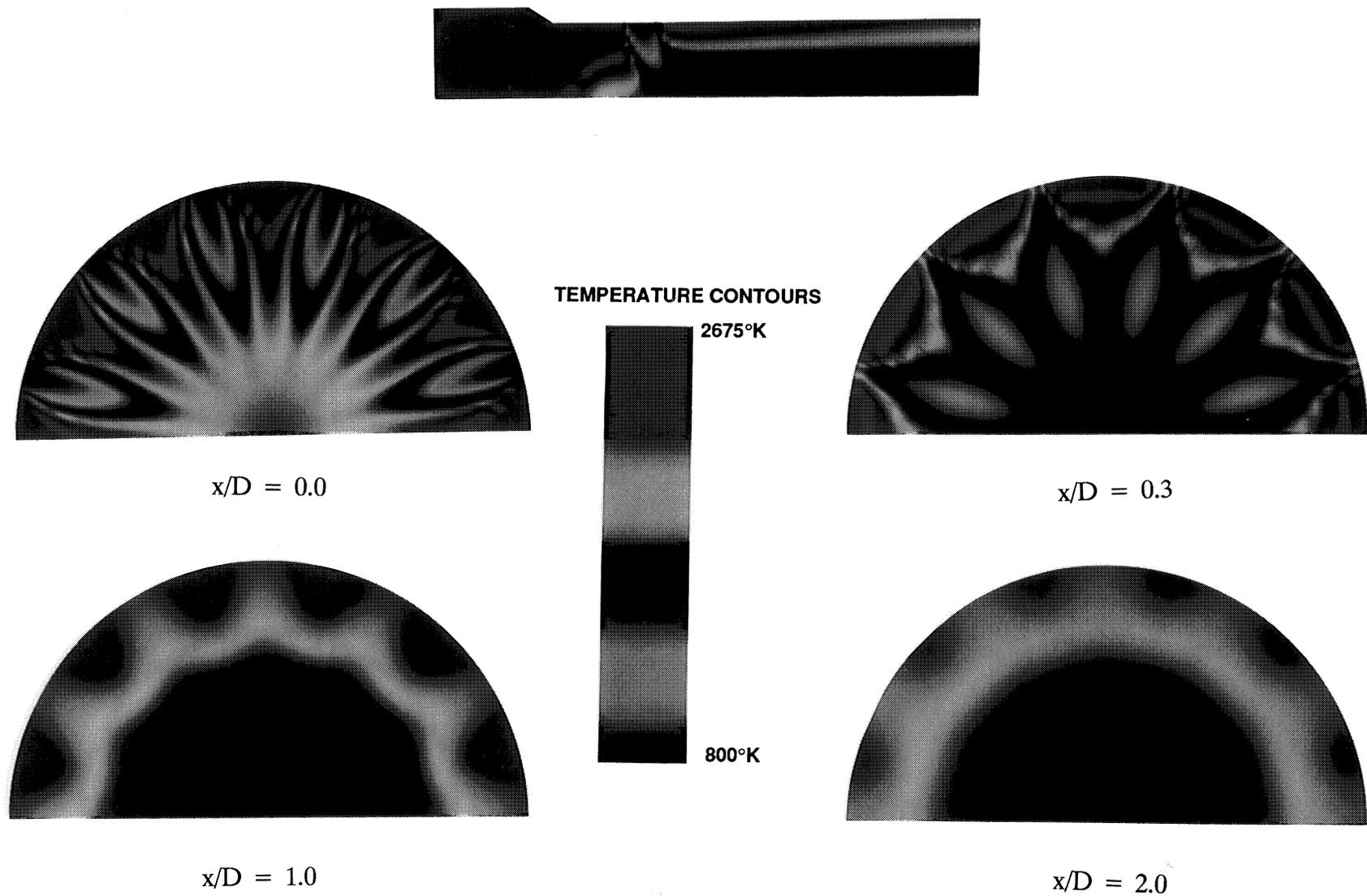
Figure A-12. Reacting Flow: J = 64 (Conventional Mixer Design)

TEMPERATURE CONTOURS

2675°K

800°K

x/D = 0.0

x/D = 0.3

x/D = 1.0

x/D = 2.0
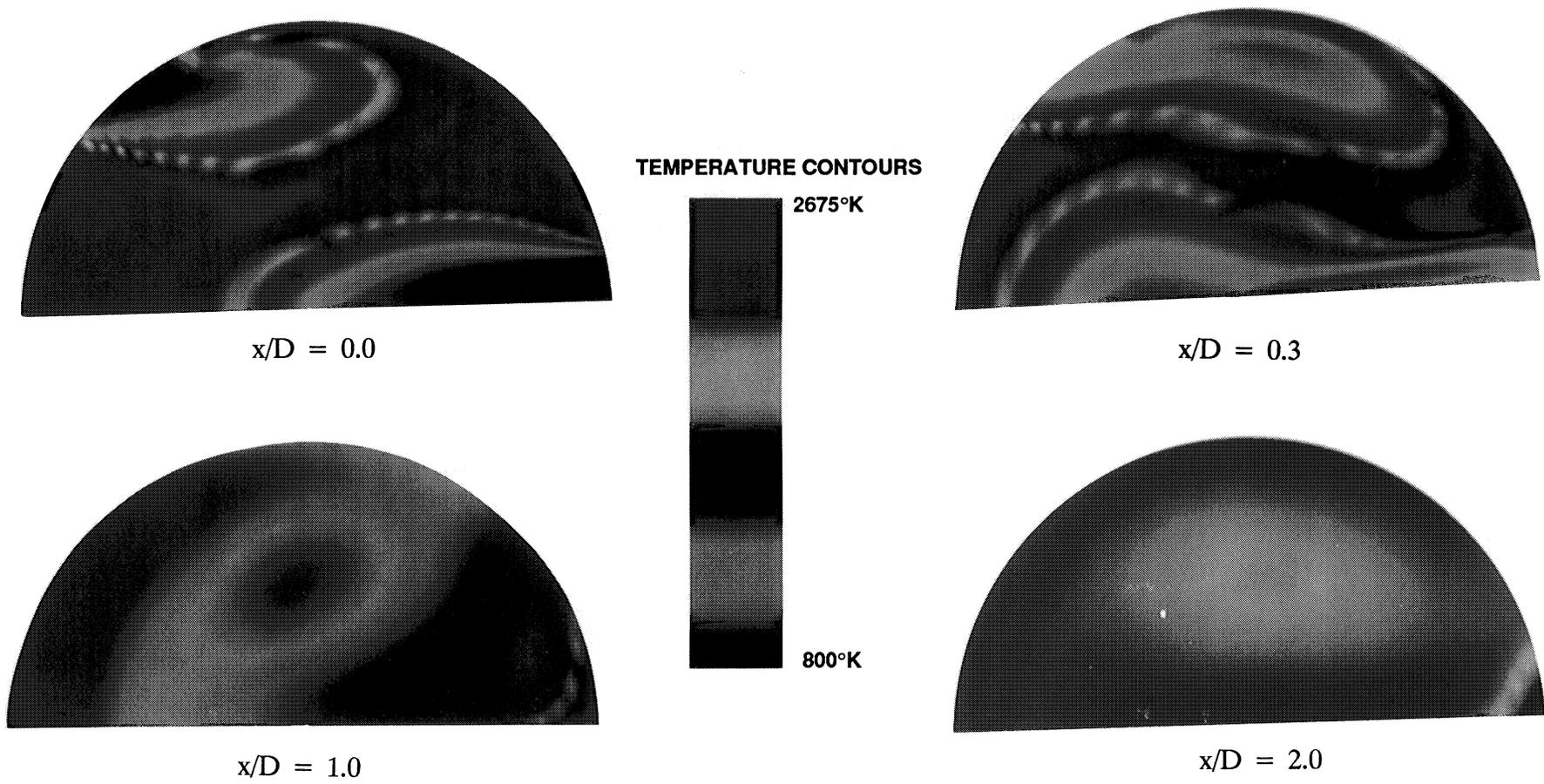
Figure A-13.   Reacting Flow: J = 32 (AJP Mixer Design, Three-Jet Case)

Report Documentation Page

1. Report No. NASA CR–185292	2. Government Accession No.	3. Recipient's Catalog No.
4. Title and Subtitle Rapid Mix Concepts for Low Emission Combustors in Gas Turbine Engines		5. Report Date October 1990
		6. Performing Organization Code
7. Author(s) Milind V. Talpallikar, Clifford E. Smith, and Ming-Chia Lai		8. Performing Organization Report No. None
		10. Work Unit No. 537–02–11
9. Performing Organization Name and Address CFD Research Corporation 3325–D Triana Blvd. Huntsville, Alabama 35805		11. Contract or Grant No. NAS3–25834
		13. Type of Report and Period Covered Contractor Report Final
12. Sponsoring Agency Name and Address National Aeronautics and Space Administration Lewis Research Center Cleveland, Ohio 44135-3191		14. Sponsoring Agency Code

15. Supplementary Notes

Project Manager, James D. Holdeman, Internal Fluid Mechanics Division, NASA Lewis Research Center. Milind V. Talpallikar and Clifford E. Smith, CFD Research Corporation; Ming-Chia Lai, Wayne State University, Detroit, Michigan 48202.

16. Abstract

NASA LeRC has identified the Rich burn/Quick-mix/Lean burn (RQL) combustor as a potential gas turbine combustor concept to reduce NO_x emissions in High Speed Civil Transport (HSCT) aircraft. To demonstrate reduced NO_x levels, NASA LeRC soon will test a flametube version of an RQL combustor. The critical technology needed for the RQL combustor is a method of quickly mixing combustion air with rich burn gases. In this SBIR project, two concepts have been proposed to enhance jet mixing in a circular cross-section: (1) the Asymmetric Jet Penetration (AJP) concept; and (2) the Lobed Mixer (LM) concept. In Phase I, two preliminary configurations of the AJP concept were compared with a conventional 12-jet radial inflow slot design. The configurations were screened using an advanced 3-D Computational Fluid Dynamics (CFD) code named REFLEQS. Both non-reacting and reacting analyses were performed. For an objective comparison, the conventional design was optimized by parametric variation of the jet-to-mainstream momentum flux (J) ratio. The optimum J was then employed in the AJP simulations. Results showed that the three-jet AJP configuration was superior in overall mixedness compared to the conventional design. However, in regards to NO_x emissions, the AJP configuration was inferior. The higher emission level for AJP was caused by a single "hot" spot located in the wake of the central jet as it entered the combustor. Ways of maintaining good mixedness while eliminating the hot spot have been identified for Phase II study. Overall, Phase I showed the viability of using CFD analyses to evaluate quick-mix concepts. A high probability exists that advanced mixing concepts will reduce NO_x emissions in RQL combustors, and should be explored in Phase II, by parallel numerical and experimental work.

17. Key Words (Suggested by Author(s)) Jets; Crossflow; Calculations; Quick mixing; RQL; Combustor		18. Distribution Statement Unclassified – Unlimited Subject Category 02	
19. Security Classif. (of this report) Unclassified	20. Security Classif. (of this page) Unclassified	21. No. of pages 72	22. Price* A04
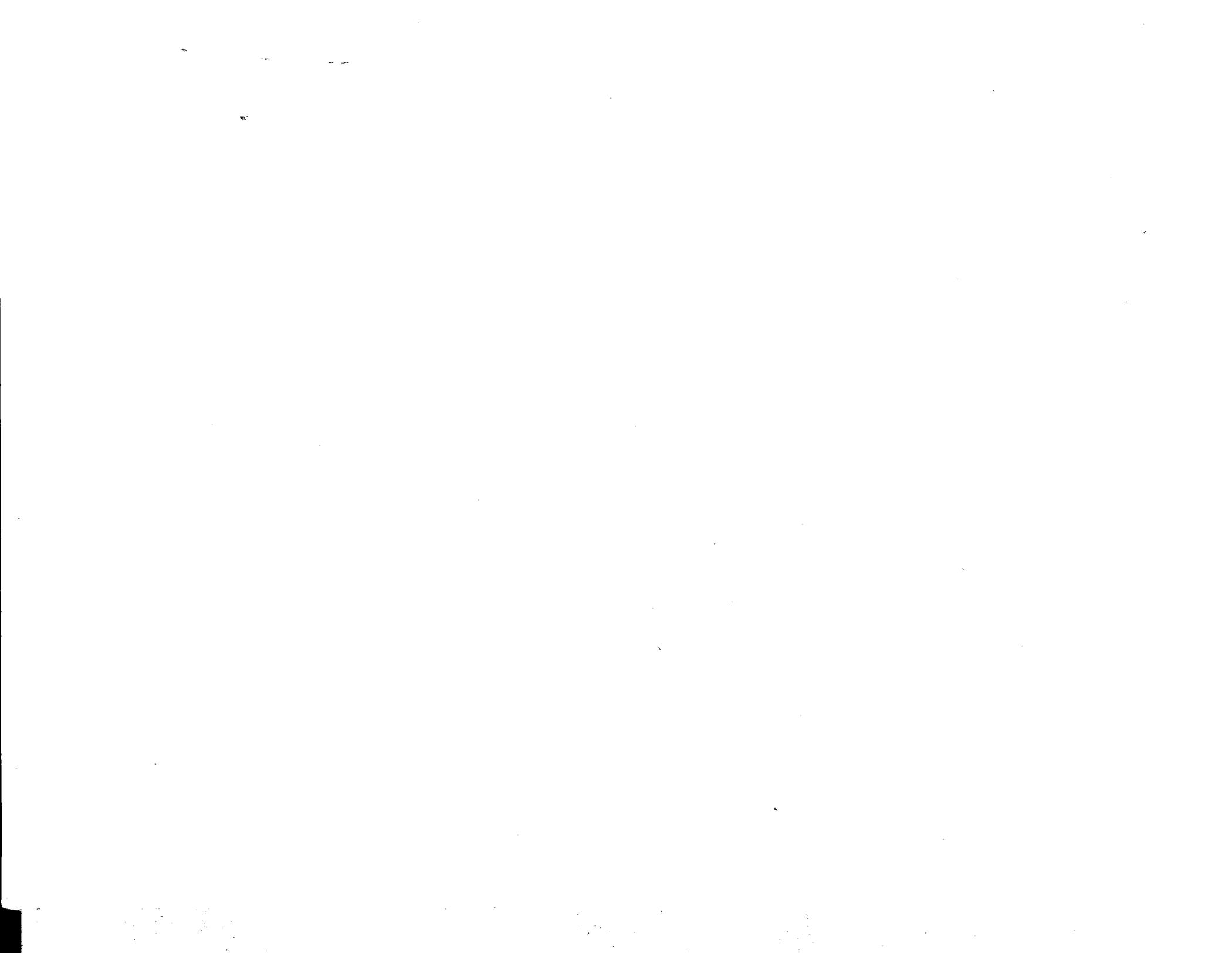
National Aeronautics and
Space Administration

Lewis Research Center
Cleveland, Ohio 44135

FOURTH CLASS MAIL

ADDRESS CORRECTION REQUESTED

NASA